The Revised Starling Principle and Its Relevance to Perioperative Fluid Management

2

C. Charles Michel, Kenton P. Arkill, and Fitz Roy E. Curry

Abstract

The Starling Principle states that fluid movements between blood and the tissue are determined by differences in hydrostatic and colloid osmotic pressures between plasma inside the microvessels and fluid outside them. While experimental evidence has established the general validity of Starling's Principle, difficulties in interpreting it quantitatively became apparent when measurements of interstitial fluid (ISF) hydrostatic and colloid osmotic pressures became possible. The revised interpretation recognizes that since vessel walls are permeable to macromolecules, a static equilibrium resulting from the balance of pressures cannot be achieved. Colloid osmotic pressure differences between plasma and interstitial fluid depend on low levels of filtration in most tissues. Plasma volume is maintained as a steady state with fluid loss by filtration from plasma to ISF being roughly matched by fluid gains from lymph. The differences in colloid osmotic pressure that determine blood tissue fluid exchange are those across the ultra-filter in vessels walls, namely the glycocalyx on the luminal surface of vascular endothelium. The mean value of colloid osmotic pressure of the ISF in a tissue can differ considerably from its value on the interstitial side of the glycocalyx since macromolecules are excluded from the main pathways through the water-filled interstices in the glycocalyx available to water and small water-soluble solutes (the small pore pathway). The macromolecules enter ISF via the

C. C. Michel (✉)
Department of Bioengineering, Imperial College, London, UK
e-mail: c.c.michel@imperial.ac.uk

K. P. Arkill
Division of Cancer and Stem Cells, School of Medicine, Biodiscovery Institute, University of Nottingham, Nottingham, UK

F. R. E. Curry
Department of Physiology and Membrane Biology and Biomedical Engineering, School of Medicine, University of California, Davis, CA, USA

E. Farag et al. (eds.), *Perioperative Fluid Management*,
https://doi.org/10.1007/978-3-030-48374-6_2

large pore pathway, which consist of very occasional openings through the endothelium and its glycocalyx (large pores) or vesicular transport. The transient changes in the rates of fluid exchange between blood and tissues are directly proportional to (linear with) transient changes in microvascular pressure. By contrast, in tissues where all the ISF is initially formed by an ultrafiltrate of plasma, the steady state levels of filtration from plasma to tissues are non-linear, being close to zero over the range of pressure below the effective colloid pressure differences and then, showing a sharp upward curvature which at higher pressures approximates closely to a straight line. In those tissues where the relation has been investigated in detail, the curve has the shape of an ice-hockey stick. The curvature (non-linearity) reflects the fact that the colloid osmotic pressure of the ultrafiltrate is dependent on filtration rate and ultimately upon the hydrostatic pressure difference. Since pulmonary capillary pressures are low, monitoring plasma colloid osmotic pressure during large crystalloid infusions may be useful in averting pulmonary edema.

Abbreviations (Where Greek characters are used, English name is given in brackets)

J_S	Solute flux
J_V	Fluid filtration rate
L_P	Hydraulic permeability (conductivity through) of microvessel wall
P	Hydrostatic pressure
P_C, P_I	Microvascular, interstitial hydrostatic pressures
P_a, P_V	Arterial, venous pressures
Π = (*pi*)	Colloid osmotic pressure
Π_P, Π_C, Π_I	Plasma, microvascular, interstitial (including sub-glycocalyx) colloid osmotic pressures
ΔP, $\Delta\Pi$ = (*delta P, delta pi*)	Hydrostatic and colloid osmotic pressure differences across glycocalyx
Ra, Rv	Pre-capillary and post-capillary resistance
σ = (*sigma*)	Membrane (osmotic) reflection coefficient
Σ = (*capital sigma*)	Summation
τ = (*tau*)	Mean transit time.

Key Points

1. Fluid movements between plasma and interstitial fluid are determined by differences in hydrostatic and colloid osmotic pressures across the glycocalyx on the luminal side of the endothelial cells. These differences in pressures are not the same as (and may differ considerably from) the differences between their mean values in plasma and interstitial fluid.

2. A static equilibrium set by a balance of hydrostatic and osmotic pressures across the glycocalyx cannot be maintained. Because microvascular walls are permeable to macromolecules, the colloid osmotic pressure difference depends on continuous filtration through the glycocalyx. In most capillaries and venules, absorption of fluid from tissues into blood is transient and reverts to low levels of filtration in the steady state. Continuous fluid uptake from tissues to blood can only occur when a significant fraction of the interstitial fluid is formed as a protein-free secretion from a nearby epithelium (e.g., intestinal mucosa, kidney cortex, and medulla) or when there is a steady flow of interstitial fluid through the tissue (e.g., lymph flowing through of lymph nodes is absorbed into the nodal microcirculation).
3. Whereas transient changes in fluid transport across microvascular walls are directly proportional to step changes in hydrostatic pressure when plasma and interstitial fluid colloid osmotic pressure are constant (a linear relation), steady state changes in fluid transport with changes in pressure are curvilinear (hockey stick shape). For increments of pressure between zero and the plasma colloid osmotic pressure, Πp, increases of steady state filtration are very small but as pressure reaches Πp, steady state filtration rates increase rapidly and approximate asymptotically to the hydraulic permeability.
4. Transient periods of fluid exchange following a step change in microvascular pressure vary considerably from tissue to tissue. A steady state is reached within a few minutes in lung, mesentery, and intestinal tract, but may take more than 30 min in skeletal muscle.
5. The hockey stick shape of the curve relating steady state fluid filtration to microvascular pressure predicts that dilution of the plasma proteins by intravenous infusion of crystalloid solutions increases fluid filtration when microvascular pressures are equal to or above plasma colloid osmotic pressure, but have little effect on steady state filtration rates when microvascular pressure is well below this (as in shock). Because pulmonary capillary pressures (Pc) are low, it suggests why moderate reductions of plasma colloid osmotic pressure by crystalloid infusions do not precipitate pulmonary edema but reducing the colloid osmotic pressure to levels just above Pc may do so.

Introduction

Intravenous fluid therapy dates from the First World War when the military surgeons were confronted by large numbers of wounded soldiers with surgical shock. Blood transfusion was experimental and difficult to carry out close to the front and the beneficial effects of infusion of crystalloid solutions (0.9% saline or 2% sodium bicarbonate solution) upon arterial blood pressure were short-lived. Following experiments on anesthetized animals by William M. Bayliss [1], the Medical Research Committee (MRC) on wound shock recommended that infusions of 0.9% saline should contain a macromolecular solute. As collaborator, colleague, and brother-in-law of Ernest H. Starling, Bayliss was, of course, familiar with Starling's

hypothesis that fluid was retained in the circulation by a balance of hydrostatic pressures and colloid osmotic pressures across the walls of capillaries [2]. In 1918, intravenous infusions of solutions of 7% gum Arabic in isotonic saline, which has the same colloid osmotic pressure and viscosity as plasma, were used to resuscitate wounded soldiers at the casualty clearing stations. It was reported to be much more effective in reducing mortality than infusions of 0.9% saline alone. Unfortunately, these reports were mainly anecdotal [3].

Although subsequent adverse reactions to artificial colloids (gum Arabic, gelatin, and dextrans) inhibited their use, it was widely believed that in the absence of blood for transfusion, infusion of plasma or isotonic salt solutions containing colloids were more effective than infusions of crystalloid solutions alone. It therefore came as a surprise when it was reported that trauma and burn patients had a lower mortality when initially treated with crystalloid infusions than when plasma or albumin solutions had been used. While the infusion of a given volume of a crystalloid solution into healthy volunteers left the circulation more rapidly than an equal volume of colloid solution, this difference was less clear when carried out in patients suffering from blood loss. The validity of the conclusions from the earliest reports were challenged and the subsequent debate—the colloid crystalloid controversy—is considered in other sections of this book.

In 2012, Woodcock and Woodcock [4] pointed out that developments over the previous 30 years in understanding microvascular fluid exchange offered a rationale for the use of crystalloid infusions in maintaining plasma volume in patients. This chapter describes these fundamental ideas, which have been called "the revised Starling Principle". First, however, we consider Starling's hypothesis as it was originally stated, the evidence for it, and how it has been misinterpreted, before moving on to discuss these more recent developments. In this chapter, the important role of the glycocalyx in fluid exchange will be discussed, but its structure, permeability, and other properties are considered in the next chapter.

Starling's Hypothesis and Its Traditional Interpretation

Starling became interested in the mechanism of lymph formation in the early 1890s. At that time, it was widely believed that lymph (tissue fluid) was formed as an active secretion of the capillary walls. Although it had been proposed that lymph was formed as an ultrafiltrate of plasma, apparently convincing evidence for lymph's active secretion had been published by Heidenhain in 1890. In 1892, Starling spent several months working with Heidenhain in Breslau (now the Polish city of Wroclaw) familiarizing himself with Heidenhain's experiments and his methods. When he returned to London later that year, he started a series of experiments in which he hoped to establish the secretory process more convincingly and show how it was regulated. The first set of experiments were carried out in collaboration with Bayliss. Far from providing convincing proof that lymph was formed as a secretion, Bayliss and Starling demonstrated that when Heidenhain's experiments were carefully controlled, they revealed powerful

evidence that lymph was formed by the ultra-filtration of plasma through the capillary walls (see [5, 6] for reviews).

At that time, it was believed that whereas fluid might be secreted from plasma into the tissues, tissue fluid could only be returned to the blood via the lymph. Convinced that interstitial fluid (ISF) was formed by the ultrafiltration of plasma, Starling now suspected that fluid could move directly from the tissues into the plasma. He assembled various lines of evidence for this, demonstrating that the fall in hematocrit after hemorrhage could not be accounted for either by an increased return of lymph from the thoracic duct to the blood or by increased uptake of fluid from the gastrointestinal tract [2]. In experiments on anesthetized dogs, where he perfused the isolated circulation of the hind limb with defibrinated blood, he then showed that a volume of 1% solution of sodium chloride injected into the muscles of the limb could be absorbed into the blood that circulated through it. An equivalent volume of plasma could not be absorbed and remained in the tissues [2]. He made the first measurements of the colloid osmotic pressure of plasma and found its value lay in the range that Bayliss and he had estimated for capillary pressures in anesthetized dogs. Here he had convincing evidence that fluid could flow directly from the tissues into the circulating blood and he proposed that the driving force for this was the difference between the colloid osmotic pressure of the plasma and that of the interstitial fluid [2].

Box 2.1 gives quotations from Starling's 1896 paper and reveals his insight in arguing that the difference in osmotic pressure between the plasma and the interstitial fluid would be proportional to the work done in forming the interstitial fluid from the plasma by ultrafiltration. He also saw his hypothesis as the principle way in which the blood volume was regulated.

Box 2.1 Starling's Hypothesis in His Own Words

"…the osmotic attraction of the serum for the extravascular fluid will be proportional to the force expended in the production of this latter, so that, at any given time, there must be a balance between the hydrostatic pressure of the blood in the capillaries and the osmotic attraction of the blood for the surrounding fluids."

"With increased capillary pressure there must be increased transudation until equilibrium is established at some higher point, when there is more dilute fluid in the tissue-spaces and therefore a greater absorbing force to balance the increased capillary pressure."

"With diminished capillary pressure there will be an osmotic absorption of saline from the extravascular fluid, until this becomes richer in proteids; and the difference between its (proteid) osmotic pressure and that of the intravascular plasma is equal to the diminished capillary pressure."

"Here then we have the balance of forces necessary to explain the accurate and speedy regulation of the circulating fluid."

From E. H. Starling *J. Physiol*. 1896 [2].

Although Starling reported improvements in his method for measuring the colloidal osmotic pressure of plasma and appreciated its importance in limiting glomerular filtration in the kidney, he published no further experimental work to support his hypothesis. He did, however, describe his ideas in the lectures that he gave and incorporated it into the textbooks of physiology that he wrote. His hypothesis was not accepted immediately and, as late as 1912, it was referred to in one influential textbook that doubted that it was the likely explanation of blood-tissue fluid exchange [6]. Some influential figures, however, were soon to be convinced. In his Silliman lectures on the capillary circulation, Krogh [7] discussed Starling's hypothesis at length but noted that nothing new had been added to the subject since Starling's paper.

Inspired by Krogh's comments, a medical student at the University of Pennsylvania, Eugene Landis, developed a method for measuring the hydrostatic pressure in single capillaries in the frog mesentery by direct micro-puncture [8]. He also developed an ingenious method for estimating the rate of fluid filtration and absorption through the walls of single capillaries. When he plotted values of the fluid filtration or absorption rates through the walls of single capillaries against the hydrostatic pressures inside them, he found a strong positive linear correlation (Fig. 2.1) [8]. When he could detect no fluid movements across the walls of a vessel,

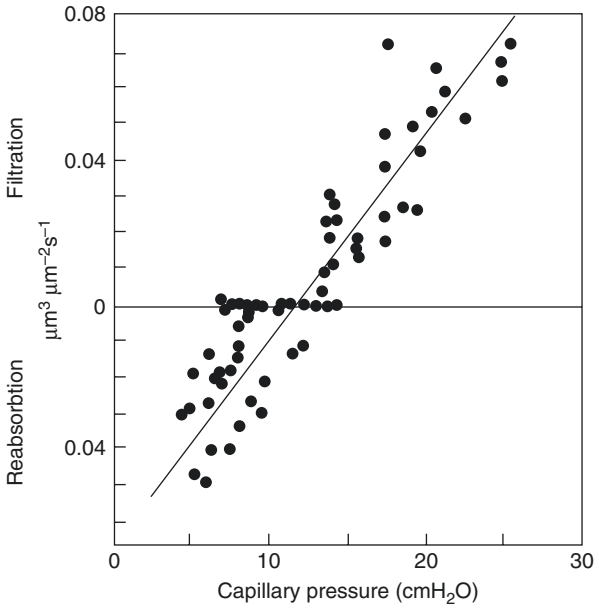

Fig. 2.1 The relationship between fluid movements through the walls of different capillaries in frog mesentery and the capillary's pressure as determined by Landis in 1927. Data re-plotted from original in *American Journal of Physiology*. (Adapted with permission of the American Physiological Society, from Michel CC. Fluid movements through capillary walls. In: *Handbook of Physiology. The Cardiovascular System.,* vol 4, *Microcirculation,* part 1, edited by Renkin EM, Michel CC, Geiger SR. American Physiological Society. 1984. Bethesda MA USA. Chap. 9, pp. 375–409

he found the capillary pressure lay within a range of values that had been measured for the colloid osmotic pressure of plasma of the same species of frogs. Landis indicated that his findings could be summarized as the equation of a linear relation between filtration rate and capillary hydrostatic pressure [8]. Using modern symbols to represent the various terms, this is:

$$\frac{J_V}{A} = L_P\left[\left(P_C - P_I\right) - \left(\Pi_C - \Pi_I\right)\right] \tag{2.1}$$

where J_V/A = filtration (+) and absorption (−) rates per unit area of capillary wall, L_P = the hydraulic permeability or conductivity of the capillary wall, P_C and P_I are the hydrostatic pressures in the capillary and the interstitial fluid respectively and Π_C and Π_I are the colloid osmotic pressures of the capillary plasma and the interstitial fluid respectively. P_C, P_I, Π_C and Π_I are often referred to as the Starling pressures.

These findings were both qualitative and quantitative evidence for Starling's hypothesis and immediately recognized as such, with Krogh rewriting the sections on the fluid exchange and permeability for the new edition of his monograph on capillaries [9].

After qualifying in medicine, Landis travelled to Europe and spent the winter of 1928/1929 in London in the laboratory of Sir Thomas Lewis. Here he measured the pressures in the capillary loops of the fingernail beds of healthy human volunteers [10]. With the subject's hand at heart level, the pressure in the arteriolar limb of the base of the capillary loops had a mean value of 32 mm Hg and in the venous limb a mean of 12 mm Hg. At the halfway point at the tip of loop, its mean value was 25 mm Hg. The colloid osmotic pressure of plasma of healthy volunteers is approximately 25 mm Hg, so this gradient of pressure along the capillaries was consistent with Starling's speculation that fluid was filtered from the plasma into the tissues at the arteriolar end of capillary beds and absorbed from the tissue spaces at the venous end [11]. (This conclusion, however, assumed that both the hydrostatic and colloid osmotic pressures of the interstitial fluid were zero).

From London, Landis moved to Copenhagen where he joined Krogh's laboratory. Here he measured capillary pressure in different tissues of the frog and small mammals. Again, he found capillary hydrostatic pressure lay in the range of values for the plasma colloid osmotic pressure measured in these different species. Not only did these findings provide further support for Starling's hypothesis, they also were consistent with Starling's conjecture [11] that fluid was lost from the circulating plasma into the tissues as it flowed through the arterial side of the microcirculation and regained fluid as the plasma flowed through the venous side. (Once again, the assumption here is that P_I and Π_I are zero.) This idea could be shown as a diagram, which was soon the standard way of teaching blood-tissue fluid exchange to medical students (Fig. 2.2). In a very influential review, Landis and Pappenheimer [12] attempted to estimate the daily flows of fluid between the arterial and venous sides of the microcirculation and the tissues. Although they recognized that microvascular walls were finitely permeable to macromolecules, they guessed that their concentrations in the interstitial fluid were very low. Although their figures have been very widely quoted, the authors themselves were cautious about conclusions

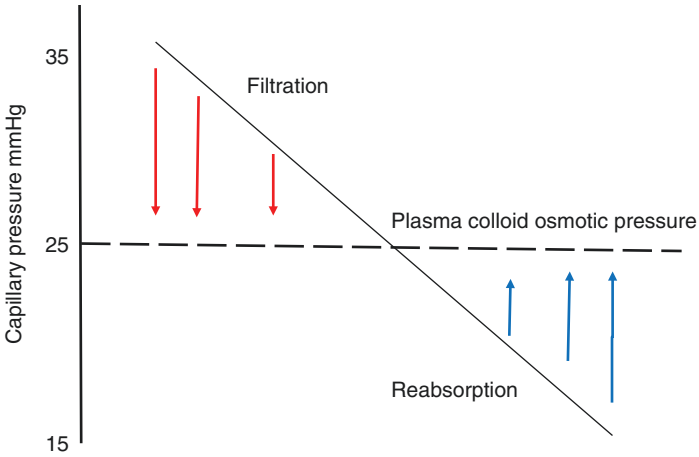

Fig. 2.2 Standard model of blood-tissue fluid exchange where filtration is shown as occurring in the upstream section of an exchange vessel where ΔP is greater than the plasma colloid osmotic pressure, and absorption is downstream where ΔP is lower than the plasma colloid osmotic pressure

drawn from them; Landis, both in this review and in his earlier writings, was well aware that the simple picture might be complicated by differences in the height of tissues relative to the heart in larger animals and particularly in humans. It was later shown that during quiet standing, P_C in the capillaries of the toes of human subjects could be 100 mm Hg or more than they were in the fingers of the same individual when the hands were held at heart level [13, 14]. As Levick [15, 34] has pointed out, there is no evidence for the textbook picture of simultaneous fluid filtration from the arterial half and fluid uptake into the venous half occurring in the microcirculation of any tissue, with the possible exception of the vasa recta of the renal medulla where other forces are involved.

Quite apart from direct measurements of capillary pressure in animals and humans, Landis's most important legacy was his demonstration of the linear relation between filtration rates and capillary pressure. He saw its importance in human physiology, developing a plethysmograph while in Krogh's laboratory for estimating fluid filtration rates in the forearm of human volunteers; he continued this approach when he returned to the United States. Here Landis and Gibbon [17] were able to show that increases in venous pressure were accompanied by increases in the rate of swelling of the tissues resulting from greater rates of ultrafiltration of fluid from the microvascular blood. If one were to assume a proportionate relationship between increments in the venous pressure and increments in the mean microvascular pressure, then their findings were consistent with Starling's Principle as expressed in eq. (2.1). More than 10 years were to elapse before the relations between arterial and venous pressures and the mean microvascular pressure in a tissue were clearly defined. Establishing these relations allowed investigators to demonstrate Starling's Principle in entire microvascular beds.

Microvascular Pressures, Vascular Resistance, and Fluid Exchange in Organs and Tissues

The relations between the mean microvascular pressure in an organ or tissue and the co-existing arterial and venous pressures was spelt out clearly by Pappenheimer and Soto-Rivera in 1948 [18]. Arguing that if the net rate of loss or gain of fluid by the blood flowing through a tissue is negligible compared with the blood flow itself, the flow of blood into a microvascular bed from the arteries is equal to the flow out into the veins. This means the blood flow from arteries to capillaries is equal to the flow of blood from the capillaries into the veins. Since flow through a section of the circulation may be expressed as the ratio of the fall in pressure across that section to the resistance to flow through the vessels, the fall in pressure from the arteries to the capillaries divided by the pre-capillary resistance should equal the fall in pressure between the capillaries and the veins divided by the post-capillary resistance. If P_a = arterial pressure, P_C = mean microvascular pressure, P_V = venous pressure and *Ra* and *Rv* are the precapillary and post-capillary resistances of the circulation, then:

$$Flow = \frac{Pa - Pc}{Ra} = \frac{Pc - Pv}{Rv},$$

which may be re-arranged as:

$$Pc = \frac{Pa + \left(\frac{Ra}{Rv}\right) Pv}{1 + \frac{Ra}{Rv}} \tag{2.2}$$

Pappenheimer and Soto-Rivera [18] worked with isolated perfused limbs of cats and dogs, which they weighed continuously to measure fluid accumulation or fluid loss from the tissues. Adjusting the arterial and venous pressures until the limb neither gained fluid from the blood nor lost it to the circulation, they argued that the mean capillary pressure in the microcirculations of the limb balanced the other pressures in the Landis-Starling equation [see eq. (2.1)] under these conditions, which they called the iso-gravimetric state. Then by adjusting the arterial and venous pressures they were able to vary the blood flow through the limb and hold the weight of the limb constant. They found that under iso-gravimetric conditions, blood flow increased linearly with reduction in the venous pressure. Arguing that in the iso-gravimetric state, the mean capillary pressure was constant, they used the linear relation between the fall in venous pressure and blood flow and determined the mean capillary pressure by backward extrapolation of the values of venous pressure to its value at zero flow when capillary pressure and venous pressure were equal. With a set of values of P_a, P_V, and P_c they could calculate *Ra/Rv* from eq. (2.2). Knowing the value of *Ra/Rv,* they could now calculate the values of P_c from the arterial and venous pressures when the limb was no longer in an iso-gravimetric state. Following this protocol, Pappenheimer and Soto-Rivera [18] were able to establish (in a mammalian preparation) nearly all the predictions made by Starling.

They were also able to demonstrate the linear relation between filtration and fluid absorption rates and mean capillary pressure (eq. 2.1) seen by Landis in frog capillaries [8]. Also, by varying the protein concentration of the plasma and adjusting the arterial and venous pressures, they showed that the mean capillary pressures, which were required to prevent net fluid gain or loss to or from the tissues, approximated very closely to the colloid osmotic pressures of the perfusates. These results suggested that, in their isolated perfused limb preparations, the interstitial hydrostatic and colloid osmotic pressures were small, being of the order of 1 to –3 mm Hg. It seemed that Starling's hypothesis had been emphatically confirmed.

The physiological importance of eq. (2.2), was demonstrated in a series of studies by Folkow, Mellander, Öberg and their colleagues in the 1960's [19–21]. They demonstrated that, in skeletal muscle, sympathetic stimulation increased R_a/R_v, leading to a fall in P_c and a shift of fluid from the tissues to the blood.

The Osmotic Reflection Coefficient

A new conceptual interpretation of osmotic pressure measurements, based on the thermodynamics of the steady state, was introduced in 1951 by A. J. Staverman [22]. He concluded that the full theoretical osmotic pressure of a solution, Π, as defined by van't Hoff (= RTC, where R = the universal gas constant, T = absolute temperature, and C = molal concentration of solute in the solution) can only be measured across a perfectly semi-permeable membrane; i.e., a membrane that is completely impermeable to the solute while being permeable to the solvent. If the membrane is permeable to the solute, the effective osmotic pressure difference across it, $\Delta\Pi$, is reduced to a value of $\sigma\Delta\Pi$. The coefficient σ is the reflection coefficient of the membrane to the solute and is a measure of the relative ease with which the solute and the solvent of a solution may pass through the membrane. For an ideal solution, σ may be defined either as the fraction of its total osmotic pressure that may be exerted by a solution across the membrane, or the fraction of solute that is separated from its solution as it is filtered through the membrane in the absence of a concentration gradient across the membrane or at an infinitely high filtration rate. The equivalence of these definitions can be appreciated intuitively by considering the osmotic pressure of a solution as the pressure that opposes its ultra-filtration through a membrane. The fraction of solute molecules that is reflected at the upstream surface of the membrane during ultrafiltration represents that fraction of the osmotic pressure of the solution opposing filtration. (This is like Starling's insight that the "attraction of the plasma for the extravascular fluid will be proportional to the force expended in the production of this latter"; see Box 2.1). If the membrane is completely impermeable to the solute but permeable to the solvent (i.e., a truly semi-permeable membrane) σ of the membrane to the solution is 1.0 and the full value of the solution's osmotic pressure opposes its ultrafiltration. If, on the other hand, the concentration of the solution leaving the downstream surface of the membrane during ultrafiltration is unchanged from that entering at its upstream surface, the membrane is unselective as an ultra-filter to the solution, $\sigma = 0$ and the

solution's osmotic pressure will not oppose its filtration. This equivalence of the definition of reflection coefficient in terms of osmotic pressure and ultra-filtration assumes that the osmotic pressure of a solution is directly proportional to the fraction of the solute molecules in the solution. This is true only for "ideal" solutions, but is a good approximation for dilute solutions where the molecular size of the solute is comparable with that of the solvent; i.e. dilute solutions of urea, glucose, and sucrose where there is a linear relation between solute concentration and osmotic pressure. For macromolecules, such as the plasma proteins, the osmotic pressures of their solutions rise more rapidly with increasing concentration, and the equivalence between the osmotic reflection coefficient and the ultra-filtration reflection coefficient is only approximate.

Because the reflection coefficients of the plasma proteins responsible for its colloid osmotic pressure are high (≥ 0.9) at the walls of microvessels in most tissues, the concept of the reflection coefficient appears in most accounts as a minor modification of eq. (2.1), i.e.:

$$\frac{J_V}{A} = L_P\left[\left(P_C - P_I\right) - \sigma\left(\Pi_C - \Pi_I\right)\right] \tag{2.3}$$

Equation (2.3) is a useful way of representing microvascular fluid exchange but, strictly speaking, it is inexact. The colloid osmotic pressure of the plasma is the sum of the products of the osmotic pressures and their reflection coefficients of all the solutes in the plasma and should be written as $\Sigma\sigma\Pi_i$ and differences of colloid osmotic pressure across microvascular walls as $\Sigma\sigma_i\Delta\Pi_i$ where subscript i represents the individual solutes that contribute to the effective osmotic pressure differences. Equation (2.3) is more accurately written as:

$$\frac{J_V}{A} = L_P\left(\Delta P - \sum_i \sigma_i \Delta\Pi_i\right) \tag{2.4}$$

where $\Delta P = P_C - P_I$.

Further development of the theory by Kedem and Katchalsky [23] led to a much clearer understanding of the relations between the rates of microvascular fluid and solute exchange, pressure and solute concentration differences and the permeability coefficients. Two examples are illustrated in Fig. 2.3 in terms of the relations between filtration rates and microvascular pressure (the Landis diagram, Fig. 2.1). Figure 2.3a shows an experiment where a single capillary has been perfused with two different Ringer's solutions [24]. The first contained 80 g/l serum albumin, but in the second solution the albumin concentration was only 25 g/l. The initial rates of fluid exchange intersect the pressure axis at approximately 30 cm H_2O when the albumin concentration is high and at approximately 12 cm H_2O when albumin concentration is low. The shift represents the difference in the effective colloid osmotic pressures ($\sigma\Delta\Pi$) exerted by the two solutions. In Fig. 2.3b, a single rat venule has been perfused *in situ* with same solution throughout an experiment [25]. Here, however, the initial measurements of filtration rates were made under control conditions. The mesentery was then treated with histamine and over the following few

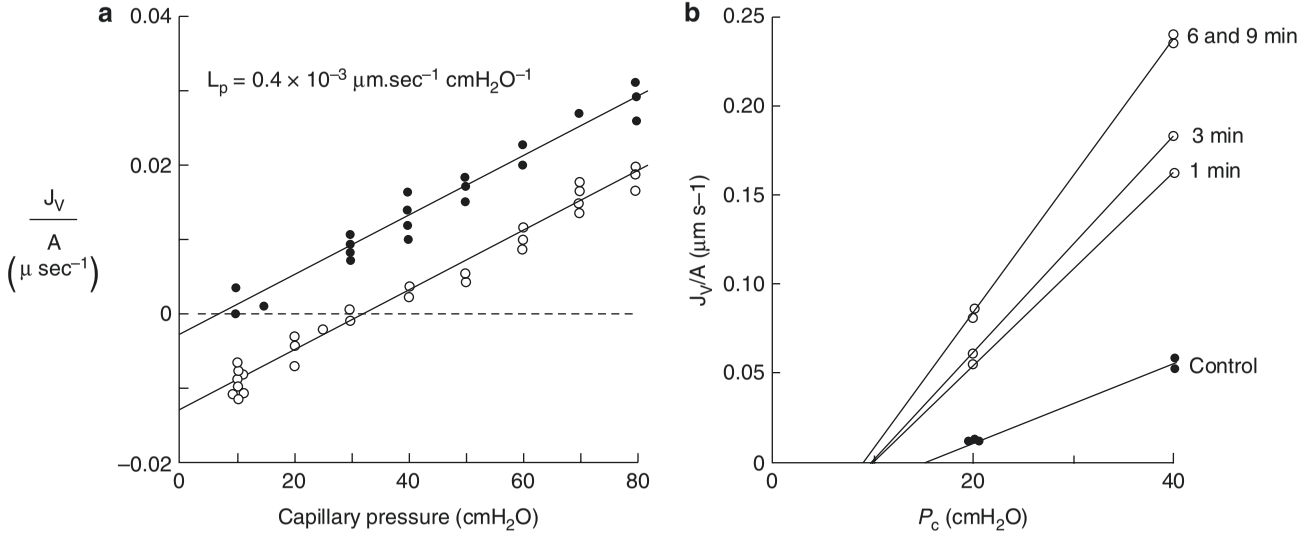

Fig. 2.3 Two experiments carried out on single perfused capillaries to illustrate the uses of the classical interpretation of Starling's principle when data are plotted in the way introduced by Landis. (**a**) The relation between fluid movements per unit area (J_V/A) and capillary pressure through the walls of a single capillary first when perfused with a Ringer solution containing 8% serum albumin (right hand line) and then with a solution containing 2.5% serum albumin. Note how reducing the albumin concentration shifts the relation to the left as the effective colloid osmotic pressure opposing filtration is reduced but the slope of the relation (hydraulic permeability) is unchanged. (Reprinted with permission of the Alfred Benzon Foundation, from Michel CC. The flow of water through the capillary wall. In: Ussing HH, Bindslev N, Lassen NA, Sten-Knudsen (eds). Alfred Benzon Symposium 15: Water Transport Across Epithelia. Copenhagen: Munksgaard, 1981: 268–279). (**b**) Changes in the relationship between fluid filtration rates per unit area (J_V/A) through the walls of a rat mesenteric venule at different microvascular pressures (P_C) before and during exposure to histamine, which increases both hydraulic permeability and permeability to macromolecules. Note how this is reflected in the increase in the slope (increased hydraulic permeability) and the leftward shift of the intercept (increased permeability to macromolecules). The numbers against each line are minutes of exposure to histamine. (Reprinted with permission from Michel CC, Kendall S. Differing effects of histamine and serotonin on microvascular permeability in anaesthetized rats. J Physiol 1997. 501: 657–662)

minutes the filtration rate rose and its relation to capillary pressure was shifted to the left indicating that the reflection coefficient of the vessel wall to the macromolecules in the perfusate was reduced. Note also that the slope of the relation between filtration rate and pressure was increased, indicating that the hydraulic permeability was increased also.

The introduction of the reflection coefficient had another important implication for the interpretation of Starling's Principle that was not immediately recognized. Until this time, it had been assumed that an equilibrium could be established between the osmotic and hydrostatic pressures differences across microvascular walls; i.e., the pressures in eq. (2.1) balance and hence zero fluid flow. The reflection coefficient was a signal that, even when the pressures were unchanging, there was no equilibrium but a steady-state could exist. This steady state was maintained by a small but steady flow of fluid from plasma to interstitial fluid to lymph. The significance of this was not appreciated for another 30 years.

The Hydrostatic and Colloid Osmotic Pressures of the Interstitial Fluids

Because the few direct measurements of capillary hydrostatic pressure that had been made before 1963 had values similar to the plasma colloid osmotic pressures and because lymph flow was low in tissues other than those of the liver and gastrointestinal tract, it was assumed that net fluid movements across microvascular walls were very low and the interstitial fluid hydrostatic and colloid osmotic pressures were small. It seemed possible that a small positive interstitial hydrostatic pressure offset the interstitial colloid osmotic pressure. The significant levels of plasma proteins found in the lymph from most tissues were believed to reflect the interstitial fluid surrounding the venules and venular capillaries where microvascular hydrostatic pressures were low. Attempts to measure interstitial fluid hydrostatic pressure by inserting a fine needle into the tissues suggested that its value was close to or slightly greater than atmospheric pressure.

In 1963, Guyton reported a novel method of estimating interstitial hydrostatic pressure (Fig. 2.4) by measuring the pressure of the fluid that accumulated in a capsule, which had been implanted and allowed to heal into the subcutaneous tissues of a dog [26]. The values he measured were between 2 and 7 mm Hg below atmospheric pressure. In later experiments, Pi measured in capsules chronically implanted in the dog lungs were found to be as low as 9–11 mm Hg below atmospheric pressure. Although soon reproduced in other laboratories, the sub-atmospheric (or negative) pressures were very controversial and there was great interest and speculation as to how they arose. Toward the end of the decade, Scholander et al. [27] reported somewhat smaller (less negative) sub-atmospheric pressures in interstitial fluids using wicks of cotton fibers saturated with isotonic saline solutions to make contact between the tissue fluids and the experimenter's manometer. Controversy as to whether the sub-atmospheric pressures were artefacts of the measuring techniques was heightened when direct measurements using the servo-nul micropipette

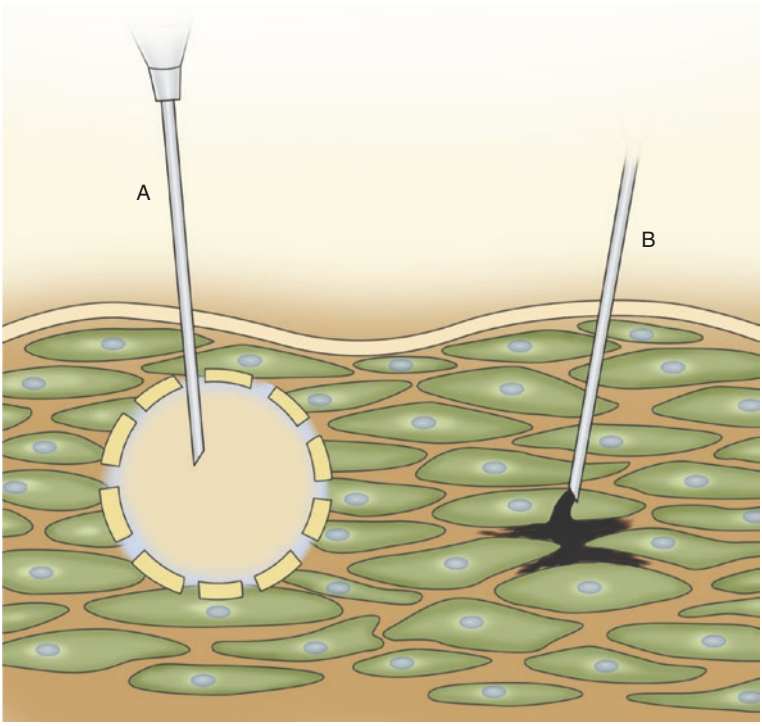

Fig. 2.4 Schematic diagram to illustrate the Guyton capsule (**a**) and the Aukland-Reed wick in needle (**b**) methods for measuring interstitial hydrostatic pressure and mean interstitial colloid osmotic pressure. Interstitial fluid hydrostatic and colloid osmotic pressures have also been measured in joint cavities and interstitial hydrostatic pressure has been measured using the servo-nul micropipette technique

technique, which had been developed to measure pressure in small blood vessels, yielded P_I values around atmospheric pressure [28].

Fluid from the implanted capsules could be removed and analyzed for its protein content and colloid osmotic pressure. A careful study by Aukland and Fadnes [29] showed that interstitial fluid protein concentration could also be obtained from implanted wicks. The values of interstitial colloid osmotic pressure, Π_I, were of the order of 10 mm Hg in subcutaneous tissues of rats and dogs. If the colloid osmotic pressure of the plasma was 25 mm Hg, this indicated that the osmotic pressure difference available to move fluid from the tissues into the plasma was only 15 mm Hg. At the same time, the sub-atmospheric values of P_I would add to the mean capillary pressure and increase the hydrostatic pressure difference favoring filtration of fluid from plasma to tissues. The direct measurements of capillary pressure, which approximated to the plasma colloid osmotic pressure and had appeared as strong evidence for a "Starling equilibrium," now seemed to suggest the differences between the hydrostatic and colloid osmotic pressures across capillary walls

amounted to 10 mm Hg or more. These implications for the concept of a balance of pressures, however, were initially overshadowed by the controversy over the measurement of P_I and what it represented.

Later, as fluid exchange came to be considered in the light of the new measurements of P_I and Π_I, the inconsistency between the few direct measurements of capillary hydrostatic pressure and the other variables of the Starling equation in the resting state led to the idea that the mean capillary pressures that determined fluid exchange were well downstream in the venular section of the microvascular beds rather than at the mid-capillary level [30–33]. The concept was reinforced by Chen et al. [31] who estimated that in order to balance the hydrostatic and colloidal osmotic pressures between the capillary blood and the interstitial fluids, the mean capillary pressure in the limb of a dog had to be as low as 12.2 mm Hg when Π_C was greater than 20 mm Hg. It was observed, however, that with small increments in interstitial fluid volume, P_I rose rapidly to zero (atmospheric pressure) and remained there as the interstitial fluid volume was increased, only rising significantly above zero after the tissues were conspicuously edematous. This, together with the older observation that increases in filtration into the tissues are accompanied by increases in lymph flow and reductions in lymph protein concentration, led to the idea that changes in the interstitial hydrostatic pressure and colloid osmotic pressure acted to minimize edema formation [31–33].

The idea that low values of the mean microvascular pressures could balance the other pressures of the Starling equation was challenged by Levick in a review published in 1991 [34]. By this time, values for the interstitial hydrostatic and colloidal osmotic pressures had been determined in many different tissues and in some cases there had also been concomitant measurements of the venular or venous pressures. Levick estimated the mean microvascular hydrostatic pressure, $P_C\,(0)$, that would balance the plasma colloid osmotic pressure and the interstitial pressures by rearranging eq. (2.3); i.e.:

$$P_C(0) = \sigma\left(\Pi_C - \Pi_I\right) - P_I \tag{2.5}$$

He then compared these values of $P_C\,(0)$ with the measured values of venous or venular pressure. His findings supplemented by a few additional values, are shown as a graph relating P_V to $P_C\,(0)$ in Fig. 2.5 [34]. Only in the intestinal mucosa and the kidney, two tissues whose specialized function is to deliver fluid and solutes into the circulation, are values of P_V below those estimated for $P_C\,(0)$. In other tissues, the higher values of P_V than $P_C\,(0)$ suggest significant levels of fluid filtration. In most of these tissues, the vascular endothelium of the capillaries and venules is continuous (non-fenestrated) and where estimates of the hydraulic permeability have been made, minimal fluid filtration rates can be calculated using the pressure differences shown in Fig. 2.5. These greatly exceed measured lymph flows from these tissues. Indeed, so large was this discrepancy that the hypothesis suggested to resolve it has been called the "revised" Starling Principle [6, 35, 36]. It involves a closer look at microvascular permeability and microvascular fluid exchange.

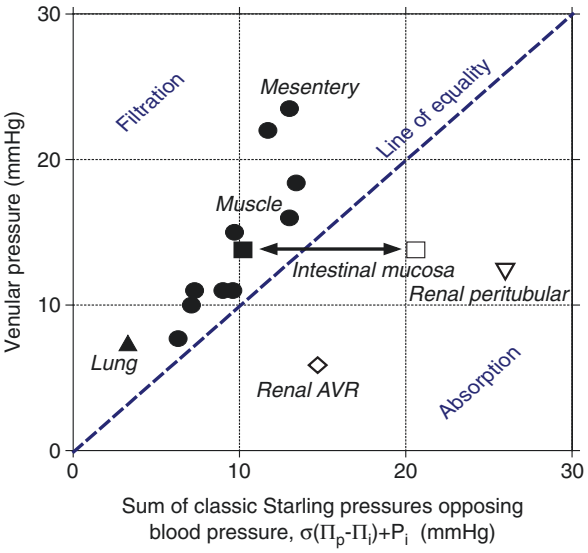

Fig. 2.5 The hydrostatic pressures in veins and venules of different tissues plotted against the sum of the pressures in those tissues that oppose fluid filtration. The Starling equilibrium or balance would be present if points lay on the line of equality. The points based on data from most tissues lie above this line indicating significant levels of fluid filtration into the tissues. Only points representing renal cortex and medulla and intestinal mucosa during absorption lie below the line. Note how the point for the intestinal mucosa lies above the line when in a non-absorptive state. (Reprinted with permission from Levick JR, Michel CC. Microvascular fluid exchange and revised Starling principle. Cardiovascular Res. 2010; 87:198–210)

Steady State Fluid Exchange Between the Plasma and the Tissues

The extension of the Starling Principle has two components. The first is the recognition of the relations between fluid exchange and microvascular pressure under steady state conditions. The second component is the hypothesis to account for the much lower filtration rates in tissues such as muscle than those that are predicted from the mean values of the capillary hydrostatic and plasma colloid osmotic pressures and the mean values of hydrostatic and colloid osmotic pressures of the interstitial fluid. In this section we consider the steady state relations.

Earlier it was noted that the concept of the reflection coefficient meant that one could no longer think in terms of the difference in hydrostatic and osmotic pressures across microvascular walls reaching an equilibrium. If microvascular walls are permeable to both proteins and water, the only true equilibrium that could be reached would be one where there were no differences in hydrostatic pressure or in protein concentration (and hence no difference in osmotic pressure) across the membrane. If a difference in hydrostatic pressure across microvascular walls is established with a higher pressure in the plasma, fluid from the plasma is filtered into the tissues and if the water molecules are able to pass more rapidly through the microvascular walls

Box 2.2 Diffusion and Convection

Diffusion is the process whereby molecules initially confined to one part of a system are able to distribute themselves throughout the system by their thermal motion. Thus, in an aqueous solution, which is concentrated in part of a region, the random kinetics of the solute and water molecules lead to net movements of solute from regions of initially high concentration to those where the concentration was initially low, exchanging places with water molecules, which show a net movement in the opposite direction. Essentially it is a mixing process on a molecular scale so that gradients of concentration are dissipated and concentration becomes uniform throughout the system with no change in volume.

Convection in this context refers to net movements of the solution (both solute and water moving together) from one part of the system to another. It is sometimes referred to as "bulk flow" or "solvent drag."

than protein molecules, a concentration difference of plasma protein across the membrane is established. The presence of a concentration difference stimulates a net diffusion of solute from plasma to tissue fluid so the maintenance of the concentration difference involves a constant race between the filtration of water molecules (convection) and the convective transport and diffusion of the solutes (Box 2.2). It requires a constant flow of fluid from the plasma into the interstitial spaces to maintain the difference in colloid osmotic pressure across microvascular walls. If the hydrostatic pressure difference is held constant for sufficient time, a steady state concentration difference develops, its value being determined by the filtration rate (and its relation to the hydrostatic pressure difference) and the relative permeability of microvascular walls to water and macromolecules.

Starling (see Box 2.1) argued that an increase in the difference in hydrostatic pressure across microvascular walls would increase filtration of fluid from plasma into the interstitial spaces concentrating the proteins in the plasma and diluting those in the interstitial fluid, so increasing the osmotic pressure difference opposing filtration. This in turn curbs the filtration rate until the latter is brought to a halt when hydrostatic pressures and osmotic pressures are equal. Starling believed at this stage a new equilibrium would be achieved, but this is not possible if microvascular walls are permeable to macromolecules.

In the absence of continued filtration, diffusion of macromolecules will dissipate their concentration difference, reducing the colloid osmotic pressure difference and allowing filtration to increase once again. For a given difference in hydrostatic pressure across the microvascular wall, however, there is a steady state difference in colloid osmotic pressure that minimizes the filtration rate. The reflection coefficient, σ, for macromolecules is high at most capillary walls and when ΔP falls below the effective osmotic pressure difference, $\sigma\Delta\Pi$, filtration in the steady state may be very low.

Figure 2.6a shows the way in which the concentration of proteins in the filtrate passing through microvascular walls varies with filtration rate when the plasma

concentration is constant. Because the reflection coefficient of microvascular walls to macromolecules is high (≥ 0.90) the protein concentration in the filtrate falls rapidly at first as filtration rate is increased and levels off to a value of less than a tenth of the plasma concentration approaching an asymptote equal to $(1\text{-}\sigma)$ multiplied by the plasma concentration. A derivation of this curve from first principles, showing its dependence on the permeability properties of microvascular walls, is given in the Appendix to this chapter.

Figure 2.6b shows how the effective osmotic pressure difference across microvascular walls varies with the filtration rate when the plasma protein concentration is held constant under steady state conditions. As one might expect from Fig. 2.6a, the effective osmotic pressure difference rises to a maximum value that is just less than the osmotic pressure of the plasma. Because the effective osmotic pressure difference, $\sigma\Delta\Pi$, is dependent upon the filtration rate, which in turn is dependent on the differences between the hydrostatic and colloid osmotic pressures, $(\Delta P - \sigma\Delta\Pi)$, the steady state relations between fluid movements and ΔP do not follow the simple linear relation that might be expected from eq. (2.3) or those shown in Figs. 2.1 and 2.3. The steady state curve predicted from the basic theory is markedly curvilinear and is shown in Fig. 2.7a [38].

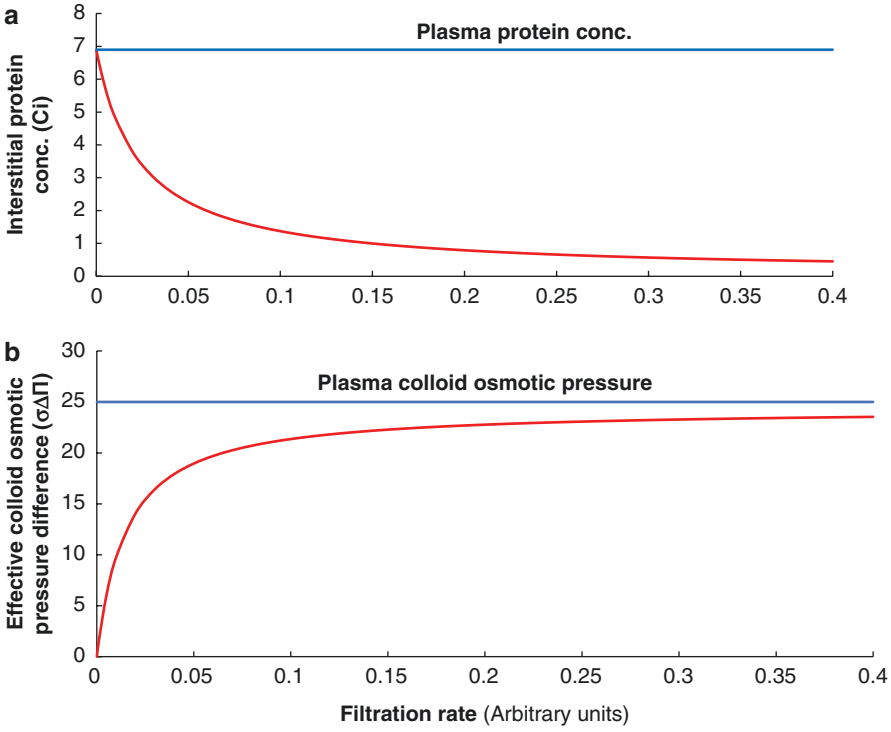

Fig. 2.6 The effects of changing filtration rate: (**a**) on steady state interstitial protein concentration and (**b**) the effective colloid osmotic pressure difference, $\sigma\Delta\Pi$, across microvascular walls. Note how $\sigma\Delta\Pi$ appears to reach a plateau at higher filtration rates

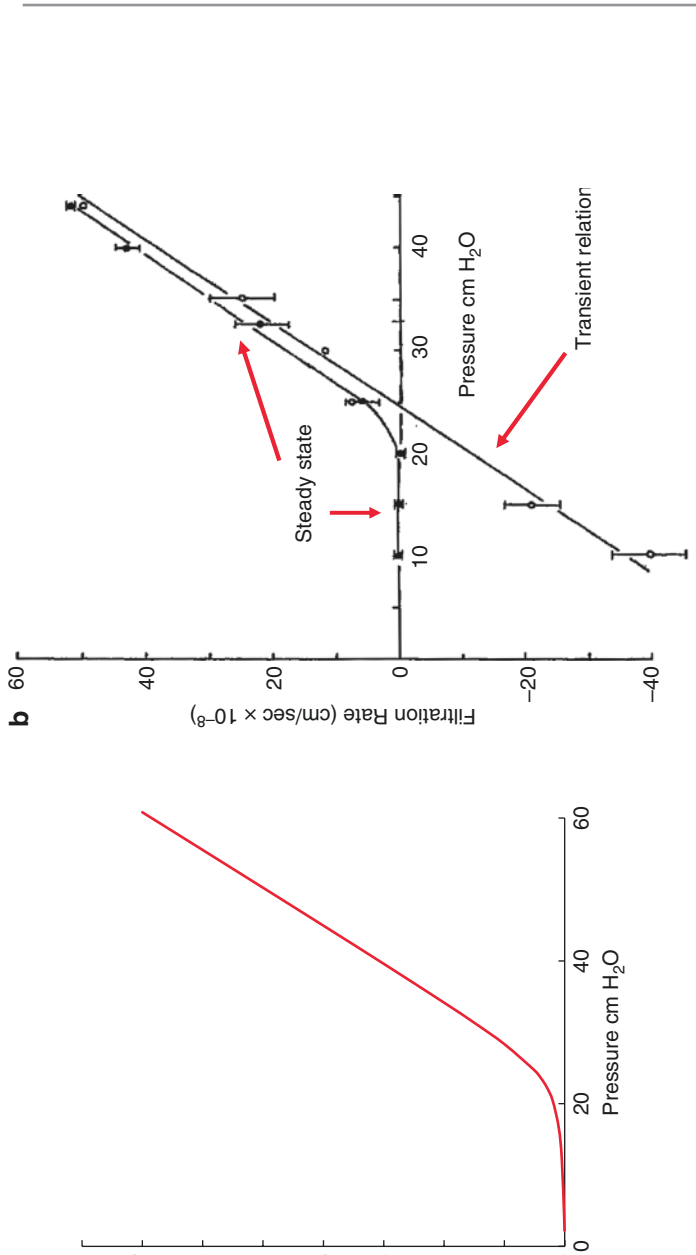

Fig. 2.7 (**a**) Steady state relations between fluid filtration rates and hydrostatic pressure difference across microvascular walls. At low pressures, steady state filtration increases only slightly with increments of pressure but as the pressure difference approaches the effective colloid osmotic pressure, filtration rate rises sharply and then increases linearly with pressure increments. This linear region develops as $\sigma\Delta\Pi$ becomes nearly constant in Fig. 2.6b. (**b**) The experiment on a single perfused mesenteric capillary demonstrating the transient and steady state relations between filtration rate per unit area of wall and capillary pressure. In this experiment the vessel was perfused initially at a high pressure (40 cm H_2O) and filtration rates measured at this pressure and then shortly after the pressure had been reduced as a step to a lower level. Steady values were then determined in the same vessel by measuring filtration rates after the vessel had been perfused at each pressure for 5–10 min. (Reprinted with permission from Michel CC, Phillips ME. Steady state fluid filtration at different capillary pressures in perfused frog mesenteric capillaries. J Physiol. 1987;388: 421–435.)

The curve was first published in a review as a way of interpreting measurements that had been reported in the literature and appeared inconsistent with contemporary interpretations of the Starling Principle in the early 1980s [32]. It departed in one conspicuous way from the traditional interpretation of Starling's Hypothesis (Fig. 2.2) in that it predicted there could be no steady state absorption of fluid into the microcirculation in tissues such as muscle, skin, and connective tissue where the interstitial fluid was formed entirely as an ultrafiltrate of the plasma. It was also inconsistent with the classical diagram for teaching Starling's Principle where there is a steady filtration from the arterial side of the microcirculation and a steady fluid uptake on the venous side.

Its general form was confirmed in experiments on single perfused microvessels, where most of the variables could be controlled with reasonable confidence (Fig. 2.7b) [37, 39]. The time course of the transient changes in fluid exchange following step changes in microvascular pressure to steady state values were also followed. The importance of making experimental investigations to check theory was underlined here, for while the experiments were able to confirm the shape of the steady state relation between fluid exchange and microvascular pressure and its relation to the transient changes, they also revealed that changes in fluid exchange from their initial values to their steady state values occurred far more quickly than was anticipated. This implied that the colloid osmotic pressure of the fluid immediately outside the exchange vessels reached their steady state values much more rapidly than the interstitial fluid as a whole. At the time it was thought that the relatively short time course of the transients was the result of slow equilibration of the proteins in the peri-vascular fluid with the rest of the interstitial fluids. Another possibility was that there were rapid changes in the interstitial hydrostatic pressure, but this seemed most unlikely in the exposed frog mesentery, which was continuously washed with a Ringer solution. Later experiments showed that in the exposed and superfused mesenteries of both frogs and rats, large changes in the filtration and absorption rates were accompanied by negligible changes in P_I when this was measured directly with a counter-pressure micropipette servo-nul system just outside the microvessels [39]. The experiment showing the change from the linear transient relation between fluid exchange and capillary pressure to the non-linear steady state relation is shown in Fig. 2.7b.

It is useful to consider that each point on the curved steady state relation between fluid exchange rate and ΔP is coincident with another linear relation that describes the transient increase in fluid exchange rate if pressure is raised or lowered. This is depicted in Fig. 2.8 where the solid curves represent the steady state relations and the parallel dashed lines are the transient relations. As mean hydrostatic pressure difference approaches and then exceeds the plasma colloid osmotic pressure, the steady state relation bends sharply upward and with further increases in ΔP the relation becomes linear and almost parallel to the transient relations. This is the stage, shown in Fig. 2.6a, b, where the concentration of plasma protein in the ultrafiltrate and the effective osmotic pressure difference across the vessel walls become nearly constant. In Fig. 2.8, we can trace how fluid exchange might change in a tissue when ΔP is suddenly reduced and remains low long enough for a new steady state to be established. Starting at point A on the steady state curve, the fall in pressure

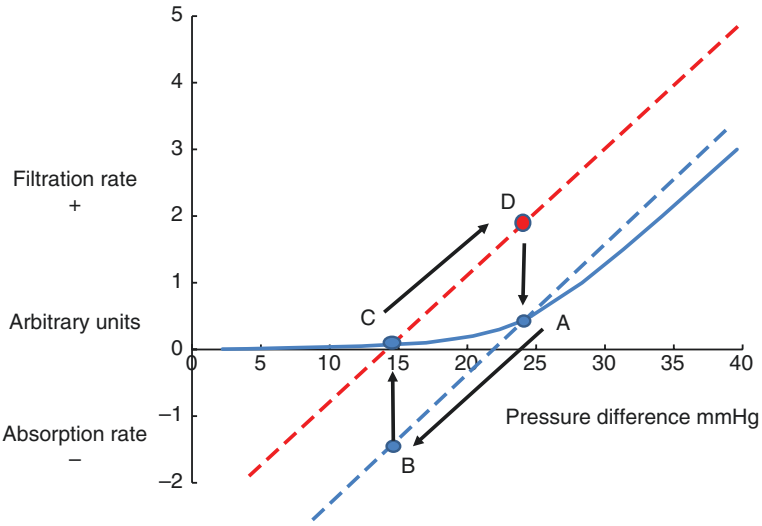

Fig. 2.8 Steady state relation between fluid movements and trans-capillary hydrostatic pressure difference (solid curve) and transient changes in fluid movement following step changes in hydrostatic pressure. Dashed lines represent transient relations (see text)

immediately moves fluid exchange from a low level of filtration to a brisk rate of fluid uptake from the tissues shown at point B. Then as a new steady state is established at the lower pressure, fluid absorption is reduced along the arrow at constant ΔP to point C where the steady state value of $\sigma\Delta\Pi$ consistent with this new level of ΔP is reached. If ΔP is now raised to its initial value, there is an immediate increase in filtration rate to point D, which is considerably greater than the initial steady state level, but this diminishes as the higher filtration rate increases $\sigma\Delta\Pi$ reducing filtration to the lower level at point A.

The rate at which a new steady state of fluid exchange is reached varies from tissue to tissue. In the pulmonary vascular bed, changes in fluid exchange rates following changes in mean capillary pressure attenuate to new steady state values within a minute or two. Here the changes in $\sigma\Delta\Pi$ are accompanied by changes in P_I, which become less sub-atmospheric (less negative) to buffer rises in P_C and more negative when P_C falls. In skeletal muscle, where initially P_C has been adjusted for fluid exchange between circulating blood and tissue to be undetectable, a subsequent step reduction in P_C is followed by brisk fluid uptake from the tissue which falls with time becoming undetectable after 30 min or more.

Steady State Fluid Uptake in Specialized Tissues

So far we have considered only those tissues where the interstitial fluid is formed entirely as an ultrafiltrate of the plasma flowing through its microcirculation and here we have concluded that there can be no continuous (steady state) fluid uptake

from interstitial space directly back into the blood. If edema is to be avoided in a tissue, the net gain of fluid by the interstitial space from microvascular filtration has to be balanced by drainage from the tissue of an equal volume of lymph. In tissues such as the cortex and medulla of the kidney and the intestinal mucosae, fluid is continuously absorbed into the microcirculation. In these absorptive tissues, the microcirculation lies close to epithelia, which secrete a protein-free solution into the interstitial fluid dominating its composition. It can be seen in Fig. 2.5 that these are the only tissues where the Starling pressures favor fluid uptake and in the case of the small intestine, this is true only during the absorptive phases. It seems that the protein-free secretion from the neighboring epithelium prevents the protein concentration from rising as fluid is absorbed into the circulation (see Fig. 2.9). The higher the rates of secretion of protein-free fluid into the ISF by the epithelium, the lower is Π_I, which increases $\sigma\Delta\Pi$ and so increases fluid uptake. In both the renal cortex and in the intestinal mucosa, lymph flow increases with absorption rates into the blood, preventing proteins from accumulating in the ISF so that steady uptake of fluid into the blood flowing through the microcirculation can continue. When the intestinal epithelium is no longer absorbing fluid and consequently not adding protein-free secretion to the ISF, fluid uptake into the microcirculation reverts to low levels of filtration (Fig. 2.5).

In the renal medulla, there are no lymphatics. Here interstitial proteins are carried directly back into the blood with the fluid that is absorbed into the ascending vasa recta. This process should concentrate the interstitial proteins, but this is

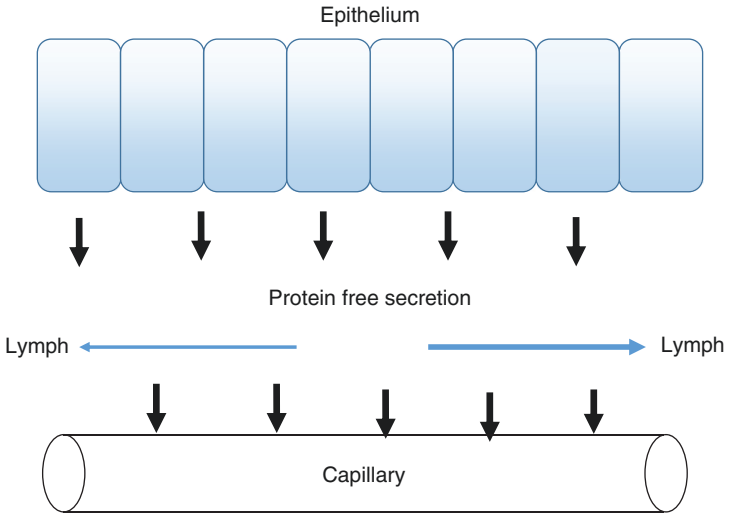

Fig. 2.9 Diagram to illustrate how the continuous uptake of fluid in capillaries of the intestine and renal cortex and medulla can be maintained by the secretion of protein-free fluid into the interstitial space from the nearby epithelium. In this way the protein concentration of the interstitial fluid can be prevented from rising and so maintains the effective colloid osmotic pressure difference across microvascular walls upon which fluid uptake depends

prevented by the continuous secretion of protein-free fluid by the epithelia of the collecting ducts and thick ascending limbs of the loops of Henle [40–42].

Steady fluid uptake also occurs into the high endothelial microvessels of lymph nodes [43]. Here the interstitial fluid is the lymph and its flow keeps protein concentration low enough for the effective osmotic pressure difference across the microvascular walls to be greater than the opposing hydrostatic pressure gradients ($\sigma\Delta\Pi > \Delta P$ in eq. 2.3).

Which Effective Colloid Osmotic Difference Is Relevant to Fluid Exchange?

Steady state fluid exchange helps us to understand why the neutral position for fluid exchange in tissues such as skeletal muscle is one of filtration. It does not, however, account for the high levels of net filtration, which may be calculated from eq. (2.4) using the plasma osmotic pressure and mean values of interstitial hydrostatic and colloid osmotic pressures in tissues such as muscle even when the venous pressure is substituted for the mean capillary pressure. Under transient conditions, the effective osmotic pressure that determines net fluid exchange is not the mean difference in pressures between the plasma and the interstitial fluid, but the hydrostatic and osmotic pressure differences across the ultra-filtering structures in microvascular walls. In experiments where the mean interstitial concentration of plasma proteins is maintained independently of the composition of the capillary ultra-filtrate, steady state differences can be maintained between the mean value of Π_I and the colloid osmotic pressure of ultrafiltrate emerging on the tissue side of endothelial ultrafilter [16]. Under physiological conditions, however, where the interstitial fluid of tissues such as skin and muscle is derived from the capillary filtrate, it is difficult to account for such large deviations (seen in Fig. 2.5) between the value of $\sigma\Delta\Pi$ across the microvascular filtering structures and that calculated from mean values for interstitial fluid and plasma under steady state conditions. The suggested solution to this question arises from the special characteristics of microvascular permeability to macromolecules.

It has been recognized for 60 years that most water and small water soluble molecules cross microvascular walls by a route that is not available to macromolecules. This pathway has been referred to as the “small pore pathway” because its permeability to water soluble molecules of differing molecular size can be modelled as diffusion and convection through a membrane penetrated by small cylindrical pores with radii of between 3.5 and 5 nm. The small pores have now been identified as the fluid-filled spaces between the fibrous molecules of the matrix that makes up the glycocalyx on the luminal surface of the endothelium. After crossing the glycocalyx of non-fenestrated endothelia, the ultrafiltrate flows through the intercellular clefts, being channeled through occasional breaks in the tight junctional strands to reach the basement membrane. To account for the permeability of microvascular walls to macromolecules, a second very much smaller population of larger pores has been proposed with radii of 15–30 nm. This is referred to as the “large pore pathway.”

Box 2.3 Aquaporin Channels in Endothelia

There is an additional pathway for water molecules that involves the aquaporin channels of the endothelial cell membranes of continuous (non-fenestrated) endothelia. This has not been convincingly shown so far to account for more than 10% of the overall hydraulic permeability. Furthermore, since it is impermeable to small water soluble molecules and ions, the role of this pathway is unclear when net flows of fluid are driven by small hydrostatic pressure gradients.

There has been much controversy as to whether the "large pores" are indeed water-filled channels through which large and small molecules are carried by convection or whether their role is played by transcytosis. There are undoubtedly specific trans-endothelial transport mechanisms for some macromolecules in some vessels (e.g., transferrin in the cerebral capillaries) but the passage of many macromolecules (including the most plentiful plasma proteins) is increased by net filtration, consistent with convective transport, and follows a general pattern consistent with their molecular size and charge (Box 2.3).

Estimation of the colloid osmotic pressure difference across microvascular walls from the protein concentrations of the plasma and their mean values in the interstitial fluid assumes that there is complete mixing of the solutions leaving the small pores and the large pores on the tissue side of the endothelial cells. The effective osmotic pressure, however, is that exerted across the membrane components of the vessel wall that act as an ultra-filter; i.e., the glycocalyx. It was realized that if mixing of the solutions leaving the small and large pores could be prevented from occurring immediately behind the glycocalyx, the effective osmotic pressure difference across the vessel wall would be increased because a larger difference in protein concentration would be present across the pathway that had the higher osmotic reflection coefficient. Figure 2.10 shows how this difference should vary with the net fluid filtration rate. It should be noted that while the increase in $\sigma\Delta\Pi$ with the channels separated is only 4 mm Hg (an improvement of 20%) the important difference is that between the curves at higher filtration rates and the plasma colloid osmotic pressure is an improvement of 75%. The difference in effective osmotic pressure here approximates to plasma colloid osmotic pressure.

How can this separation of the downstream effluents from the two pathways be achieved? The deviations from a balance of the pressures revealed by Levick's analysis [34] showed that it was most significant in those microvessels where the endothelia were continuous (non-fenestrated). For these vessels the same possible mechanism for separating the flows was suggested independently by Michel [6] and Weinbaum [44]. Plasma ultrafiltrate, which is formed by flow through the glycocalyx at the luminal endothelial surface, has to pass by a tortuous route through infrequent breaks in the tight junctional strands of the intercellular clefts of the endothelium to reach its abluminal surface and the basement membrane (Fig. 2.11) [38]. The structural equivalent of the large pores are possibly very rare open intercellular clefts or channels formed by fused vesicles that pass directly through the endothelium to its abluminal surface. Macromolecules passing through these

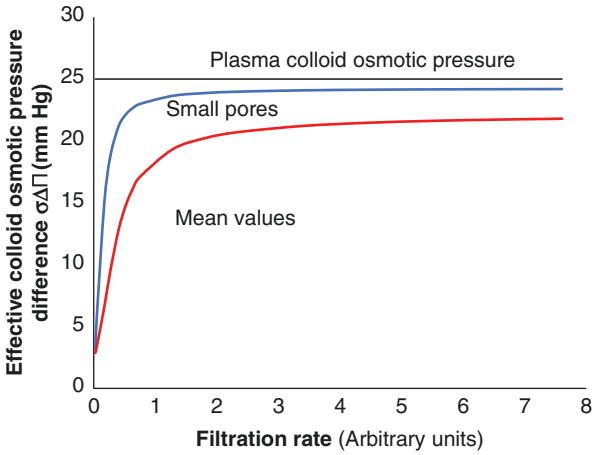

Fig. 2.10 Steady state relations between the effective osmotic pressure difference across skeletal muscle micro-vessels and fluid filtration rates comparing the mean values with those across the small pores (glycocalyx). Note how the effective osmotic pressure difference seen across the small pores (glycocalyx) approximates more closely to the plasma colloid osmotic pressure than the mean difference. The difference between $\sigma\Delta\Pi$ and Π_P across the small pores is a quarter of that based on mean values

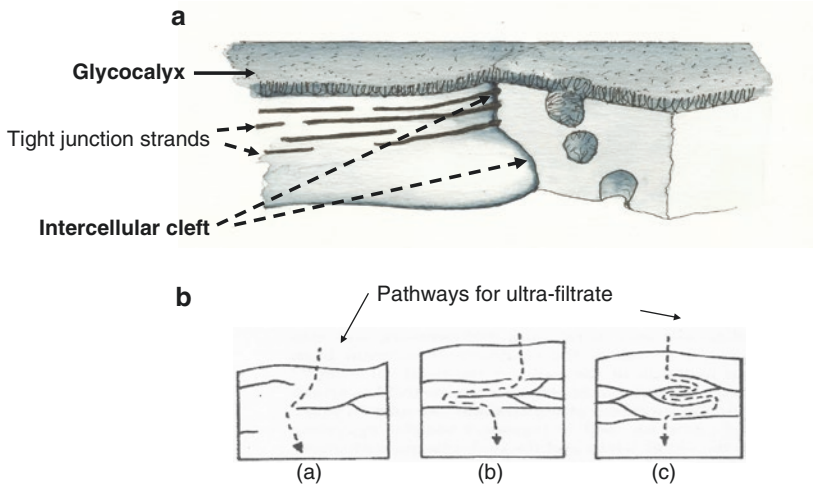

Fig. 2.11 Diagrams to illustrate the ultrastructure within an intercellular cleft between endothelial cells and the pathways through them for water and small hydrophilic solutes that have passed through the glycocalyx. (**a**) Part of the cell in the foreground has been removed to display the cleft interior. Note the junctional strands and the potential pathways through the breaks in them. (**b**) After flowing through the glycocalyx, which excludes macromolecules, the ultra-filtrate enters the luminal section of the intercellular cleft and is diverted to where there are breaks in the first tight junctional strand. The dashed lines with arrows indicate the potential pathways through intercellular clefts in different capillaries: (a) mesenteric capillary; (b) cardiac muscle capillary; (c) skeletal muscle capillary. (Reprinted with permission from Michel CC. Exchange of fluid and solutes across microvascular walls. In: Seldin DW, Giebisch G (eds). The Kidney: Physiology and pathophysiology. Vol 1. 2000. Philadelphia, Pennsylvania, USA: Lippincott, Williams &Wilkins. 2000: p 61–84)

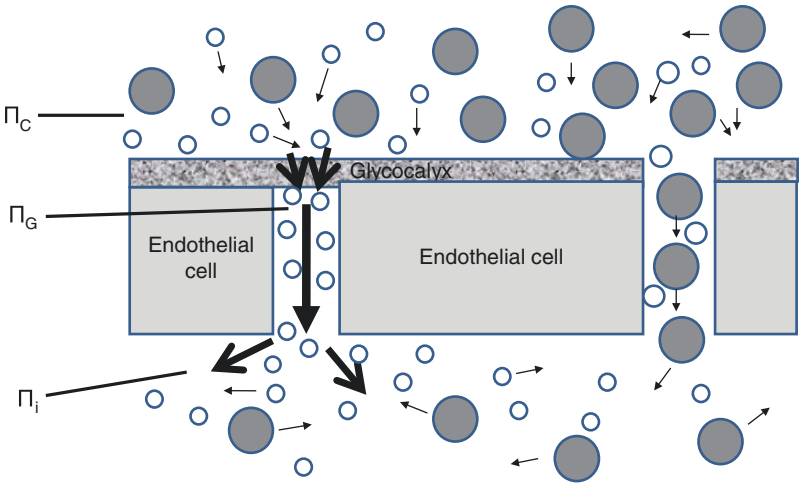

Fig. 2.12 A schematic diagram of fluid and protein exchange across walls of microvessels with continuous (non-fenestrated) endothelia. Small open circles represent water molecules; large filled circles represent protein molecules, with the plasma shown above the endothelium and the interstitial fluid below. Water crosses the endothelium through the intercellular clefts (left of picture) after having passed through the glycocalyx which filters out the protein (the small pores). Proteins cross by the large pore to the right of the picture below an opening in the glycocalyx. Large pores are relatively few (one per 10,000 small pores). The thickness and length of the arrows indicate the mean velocities of the molecules. Because the velocity of the water molecules in the intercellular clefts in amplified by 1–4 orders of magnitude, it prevents protein molecules from back diffusing up the clefts to the underside of the glycocalyx. (Reprinted with permission from Michel CC. Microvascular fluid filtration and lymph formation. In: Santambrogio L (ed). Immunology of the lymphatic system. New York: Springer, 2013: p 35–51)

channels from the plasma may be expected to arrive at the basement membrane and equilibrate with fluid there, most of which will have been filtered through the glycocalyx before passing through the intact intercellular clefts. In the absence of flow through the clefts, plasma proteins may be able to diffuse back through the breaks in the tight junctions to reach the underside of the glycocalyx. But calculations indicate that in the presence of even a low level of filtration through the intercellular clefts, such as might result from a difference in ΔP of as little as 1 cm H_2O, it is unlikely that proteins such as serum albumin would be able to back diffuse from the basement membrane beyond the tight junction. This is because the flow velocity of the filtrate as it leaves the underside of the glycocalyx is amplified many times over as it is funneled through the breaks in the junctional strands, which form the tight junctions. These openings constitute no more than 10% of the length of the clefts in the most permeable microvessels with continuous endothelium and in mammalian skeletal muscle, the freeze-fracture studies of the junctional strands suggest an open fraction of closer to 1%, which would increase the flow velocity of the fluid 100 times more than its velocity upon entering and leaving the intercellular clefts. Detailed modeling of this effect suggested that back diffusion of protein to the underside of the glycocalyx would be even less likely than initial rough calculations had indicated. The hypothesis is summarized in Fig. 2.12 [45].

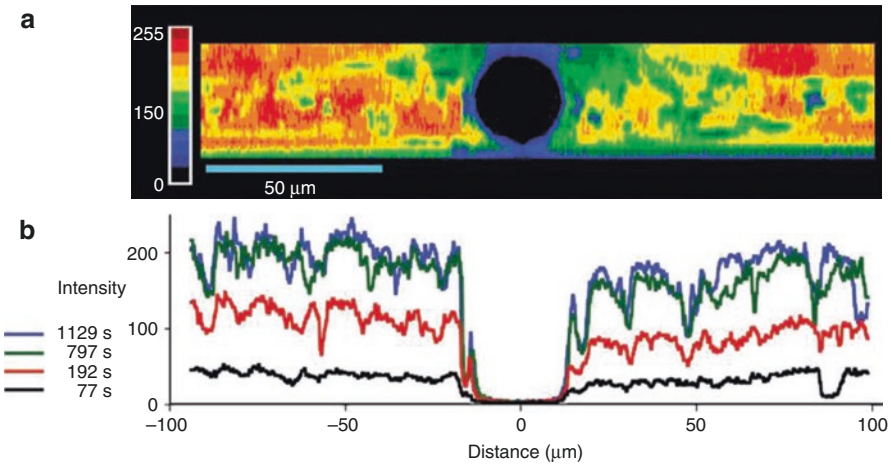

Fig. 2.13 Serum albumin concentration gradients around a venule in the rat mesentery at various times after fluorescently labeled albumin has been added to the superfusate. (**a**) Fluorescence image of a transverse section through the vessel and surrounding tissue. The vessel is perfused with an unlabeled albumin solution at the same concentration as the labeled albumin in the superfusate and appears as a dark circle. (**b**) Intensity profiles, taken from images such as that shown in (**a**), showing how the concentration in the tissue builds with time, taking between 12 and 20 min to a reach a steady state. It is seen that the interstitial albumin concentration in this experiment is equal to that in the superfusate within one μ(mu)m of the vessel lumen. (Reprinted with permission from Adamson RH, Lenz JF, Zhang X, Adamson GN, Weinbaum S, Curry FE. Oncotic pressures opposing filtration across non-fenestrated rat microvessels. J Physiol. 2004; 557: 889–907)

Shortly after this hypothesis was proposed, Curry suggested an experiment to test it. If the interstitial space is loaded with protein to the same concentration as that present in the plasma, it should only influence filtration rates through capillary walls when the microvascular pressures were below the plasma colloid osmotic pressure. This was soon shown to be so, first in single perfused capillaries of the frog mesentery [46] and later in rat mesenteric venules [47]. Figures 2.13 and 2.14 are taken from the paper by Adamson et al. [47]. In each experiment, a single microvessel was perfused *in situ* through a micropipette with a Ringer solution containing 5% serum albumin while the exposed surface of the mesentery was washed initially with a protein-free Ringer solution (the superfusate). The relations between fluid filtration rates and microvascular pressures were determined for the vessel and the effective osmotic pressure exerted by the perfusate opposing filtration was determined.

The superfusate was then changed to one that was identical to the perfusate in all respects except here the albumin was fluorescently labelled so its presence in the tissues could be monitored. When the fluorescent intensity of albumin surrounding the perfused capillary had reached the level indicating that its concentration was equal to that inside the vessel, the relations between the fluid filtration rates and microvascular pressure was re-determined. Under these conditions, one might

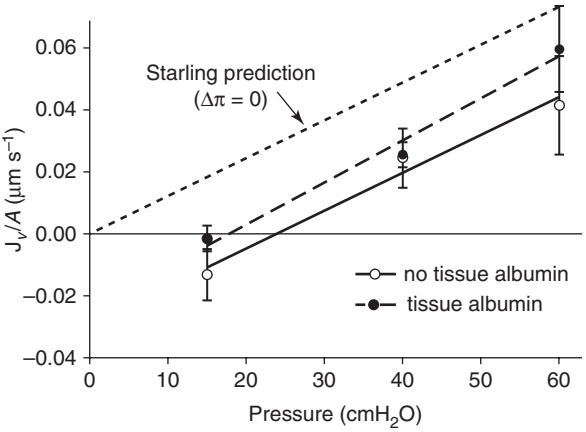

Fig. 2.14 Transient relations between filtration rates from a rat venule and microvascular pressure perfused with a solution containing serum albumin (50 mg/ml) when the superfusate washing the surface of the mesentery contains no albumin (open circles) and the same albumin concentration as that in the solution perfusing the vessel (closed circles). Measurements of filtration rates were made when there appeared to be no difference in albumin concentration across the vessel walls. The classical interpretation of Starling's principle would predict the relation should pass through the origin of the graph. The large intercept at $J_V/A = 0$ indicates a substantial colloid osmotic pressure still opposes filtration. (Reprinted with permission from Adamson RH, Lenz JF, Zhang X, Adamson GN, Weinbaum S, Curry FE. Oncotic pressures opposing filtration across non-fenestrated rat microvessels. J Physiol. 2004; 557: 889–907)

expect that the effective osmotic pressure opposing filtration from the vessel would now be zero. Where, however, pressure was several cm H_2O above the colloid osmotic pressure of the perfusate, the effective osmotic pressure opposing filtration was very little less than it had been when the superfusate contained no protein. Furthermore, as shown in Fig. 2.14, the transient changes in filtration rate when microvascular pressure was dropped to lower levels remained unchanged. Only when the vessel was perfused at low levels for a few minutes did the effective osmotic pressure opposing filtration diminish. The experiments clearly demonstrate how the effective osmotic pressure difference across microvascular walls may be independent of the mean colloid osmotic pressure of the interstitial fluid. Furthermore, the changes in filtration rates with pressure are entirely consistent with the prediction of the Michel-Weinbaum hypothesis, strengthening its claim as an explanation of low filtration rates consistent with local lymph flows.

This series of experiments also confirmed the validity of the steady state theory and like the earlier experiments of Michel and Phillips [37] found that the transition from transient to steady state fluid exchange occurred very much more quickly than would be expected if it involved the entire interstitial fluid of the tissue equilibrating with microvascular filtrate. Electron microscopy of mesenteric microvessels reveals that these vessels are closely sleeved by pericytes. It was argued that the narrow spaces between the abluminal surface of the endothelial cells and the

pericytes act as a compartment or "micro-domain," which equilibrates quickly with the capillary filtrate, rapidly increasing the rate at which a new steady state is established [48].

A Picture to Forget

A popular textbook diagram to illustrate the Starling Hypothesis depicts a linear fall in pressure along a capillary with its value at the arterial end in the range of 35 mm Hg and with the venous end around 15 mm Hg (Fig. 2.15a). This sloping line crosses the horizontal line, which indicates the colloid osmotic pressure of the plasma of 25 mm Hg. In the space between the lines when pressure is greater than 25 mm Hg, a series of downward pointing arrows indicate fluid being filtered from the vessel into the tissues; over the second half of the capillary when pressure is less than 25 mm Hg, the arrows point upward, indicating the uptake of fluid from the

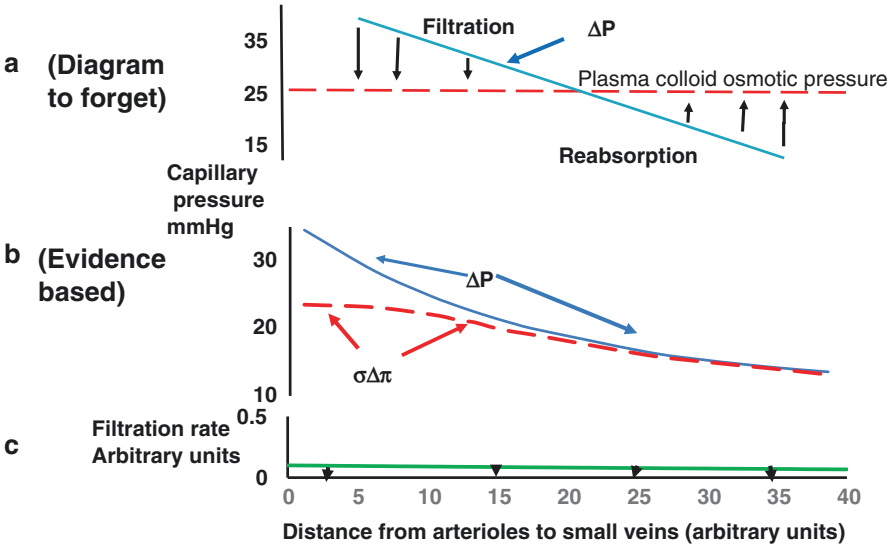

Fig. 2.15 (**a**) Version of the widely used textbook diagram to illustrate Starling's Hypothesis with filtration occurring in the upstream section of an exchange vessel where $\Delta P >$ plasma colloid osmotic pressure, Π_p, and absorption downstream where $\Delta P < \Pi_p$. Interstitial colloid osmotic pressure is incorporated by subtracting its mean value from Π_p at all points along the vessel. (**b**) Changing values of ΔP and $\sigma\Delta\Pi$ across the microcirculation of a tissue such as skeletal muscle under steady state conditions consistent with revised Starling Principle. $\Delta P > \sigma\Delta\Pi$ at all points although difference is less than 1 mm Hg for a majority of vessels. If net filtration were indicated by arrows drawn between the curves for ΔP and $\sigma\Delta\Pi$ as in (**a**), its low near constant value across the microcirculation would not be conveyed. (**c**) When differences in exchange surface area and L_P are taken into account, near constant filtration into the tissues consistent with $\Delta P - \sigma\Delta\Pi$ is achieved as expected

tissues. This diagram has been remarkably successful in enabling medical students to satisfy their examiners with their understanding of blood-tissue fluid exchange. Attractive though it is, the diagram implies several things for which there is no experimental evidence and are probably never true.

The diagram suggests that it represents the net fluid movements in a typical microcirculation such as that of skin or muscle. Quite apart from there being no evidence that both filtration and absorption occur simultaneously in these microcirculations (see later), it would be atypical of most vascular beds for it implies that the exchange vessels are present in equal numbers at the arterial and venous ends of a microcirculation and are also of equal permeability to fluid and macromolecules. Arterioles, arteriolar capillaries, mid-capillaries, and venules are all recognized to be involved in the blood-tissue exchange of solutes. In the arterioles, exchange is probably confined to the respiratory gases with fluid exchange occurring to some degree in all the other exchange vessels downstream. There are more mid-capillaries than arterial capillaries resulting in an increase in the surface area of the vessel walls available for exchange. The exchange area is further increased by an increase in vessel radius as one moves to the venular capillaries. In most tissues, the wall surface area is maintained in the small venules where a reduction in the number of vessels is compensated for by an increase in vessel diameter. There are two obvious consequences. First, the fall in hydrostatic pressure is greatest between arterioles and mid-capillaries and becomes progressively less steep as one passes through the microvascular bed toward the veins; this has been demonstrated very clearly in microcirculations of mesentery and skeletal muscle [49]. Second, the increase in area available for exchange means that even if the hydraulic permeability were the same in all exchange vessels, a small difference in pressure across vessel walls at the venous end of the microcirculation has greater net effect on fluid exchange than it would have at the arterial end. Also, where measurements of L_P have been made in single vessels, L_P has higher values in venular capillaries and venules than in vessels upstream. If this arterio-venous gradient of L_P is present in most microvascular beds, it will multiply with the increasing area for exchange and be consistent with the conclusion reached earlier: that microvascular fluid exchange occurs mainly in the region of the venular capillaries and venules.

An obvious criticism of Fig. 2.15a is that it ignores, Π_I, the colloid osmotic pressure of the interstitial fluid. We have seen that Π_I cannot be taken as a constant that can be subtracted from the plasma colloid osmotic pressure. For the revised Starling Principle, the colloid osmotic pressure difference, which influences fluid exchange, is that across the glycocalyx. This varies with the filtration rate and ultimately with the hydrostatic pressure difference across the vessel wall. As we have seen, the colloid osmotic pressure underneath the glycocalyx can differ considerably from the mean colloid osmotic pressure of the ISF. To illustrate this for a microcirculation such as that in skeletal muscle, the hydrostatic pressure difference, ΔP, and the effective colloid osmotic pressure difference, $\sigma\Delta\Pi$, have been plotted against the distance from the arteriolar capillaries to the larger venules in Fig. 2.15b. The nonlinear fall in ΔP is shown as the upper curve and the lower curve is $\sigma\Delta\Pi$, estimated for steady state conditions of fluid exchange. Whereas the difference $(\Delta P - \sigma\Delta\Pi)$ is

initially more than 10 mm Hg, it is soon reduced to 1 mm Hg and continues to fall to less than this. The largest differences in pressure driving fluid from plasma to tissue are seen in the arteriolar capillaries, which contribute least to the exchange area of the microvascular bed. Probably they also have the lowest values of L_P and so the net movement of fluid from blood to tissue from this part of the microcirculation is relatively small. This is illustrated in Fig. 2.15c, which shows a low and almost constant level of fluid filtration from the plasma as it flows through the microvascular bed.

The low level of filtration represents the steady state condition in microcirculations of tissues such as muscle. These low levels of filtration are expected in muscle tissues when subjects are supine and P_C lies in the range of 15–35 mm Hg, but most of the daytime of healthy subjects is spent standing, sitting, and walking when most of their body lies below heart level and when P_C is both variable and considerably higher than this range [13, 14, 32]. These conditions do increase interstitial volume in the lower parts of the body and increase the lymph flow from them [50]. Some of this additional extravascular fluid will be absorbed directly into microcirculation during the first hour of bed rest, but probably more is absorbed from the lymph as it flows through the lymph nodes. Independent studies by Adair et al. [43] and Knox and Pflug [51] demonstrated that the protein concentration of post-nodal lymph was on average twice that in pre-nodal lymph. Both groups investigated lymph flows through the popliteal nodes of anesthetized dogs. Estimates of the pre-nodal and post-nodal lymph flows by Adair et al. [43] indicated that the doubling of protein concentration in the post-nodal lymph was accompanied by a halving of lymph flow, indicating that half the pre-nodal flow was absorbed into the blood flowing through the node. Knox and Pflug [51] noted that the ratio of concentrations in the post-nodal lymph to those in the pre-nodal lymph was the same for all proteins and independent of their absolute values. From this they concluded that higher concentrations in the post-nodal lymph were consistent with fluid removal from the lymph as it flowed through the node rather than by the addition of protein to the lymph. Further experiments in which labelled albumin was injected directly into the pre-nodal lymph confirmed this interpretation [51]. Because lymph flows through the nodes and continually renews the fluid outside the blood capillaries and venules, steady state fluid uptake can occur here. Its importance can be appreciated if we make rough estimates of the volume of fluid filtered daily from plasma into the total muscle mass of a human subject.

Skeletal muscle mass of a 70 kg male subject is approximately 28 kg and estimates of the product of L_PA for soft tissues of the forearm and calf regions, which are largely muscle, lie in the range of 0.0025 to 0.004 ml min^{-1} mm Hg^{-1} 100 g^{-1} of tissue. Using the difference $(\Delta P - \sigma\Delta\Pi)$, as shown in Fig. 2.15b, and averaging it over the exchange area of the muscle microcirculation leads to a mean value of just less than 1 mm Hg. Using these values, one calculates a net daily filtration of between 800 ml and 1300 ml. These figures represent the basal levels that might occur during sleep (or bed rest) and additional volumes of fluid filtered into muscles of the lower half of the body during sitting or standing would probably double these figures. If during the first hour or so of bed rest transient absorption of fluid was

driven by a mean pressure of 2 mm Hg, 100–300 ml of extravascular fluid might be absorbed directly into the circulation. A further 800–1300 ml would be absorbed from the lymph flowing through regional lymph nodes over 8 h of bed rest and possibly a similar volume during the daytime. This would mean that of the 1600–2600 ml of fluid filtered into skeletal muscle during a day, between 900 ml and 1600 ml would be absorbed mostly at the lymph nodes leaving a remaining volume to be added to thoracic duct lymph of between 700 ml and 1 L. The estimates of the thoracic duct lymph flow in human subjects have been restricted to a few measurements made on patients with thoracic duct fistulae and are approximately 4 L per day in non-fasting subjects when two-thirds of the lymph is derived from the liver and gastrointestinal tract. Since skeletal muscle constitutes 40% of the total body mass, a contribution of approximately 20% to thoracic duct lymph seems reasonable. This is a rather more realistic figure than that to which Levick [34] drew attention 29 years ago. Following the argument implied in Fig. 2.15a, by subtracting mean ISF Π_I from Π_P, Bates et al. [52] found that ($\Delta P - \sigma\Delta\Pi$) exceeded the **venous** pressure in human forearm skeletal muscle by 4–5 mm Hg. Because the mean capillary pressure is likely to be 5–15 mm Hg greater than the venous pressure, the net pressure driving filtration throughout the microvascular bed could be as high as 10 mm Hg. Even if it were only 5 mm Hg and also that both the patient remained supine and half the fluid filtered into 28 kg muscle were absorbed in the lymph nodes, there would remain 6 L of fluid to be added to thoracic duct lymph every day; i.e., 150% of the maximum estimates for the sum of the daily flows for both thoracic duct and right lymph ducts. However useful Fig. 2.15a may have been as an *aide mémoire*, it is misleading and cannot be used for clinical decision making. Figure 2.15b is much closer to the truth.

Relevance of the Revised Starling Principle to Intravenous Fluid Therapy

Woodcock and Woodcock [4] drew attention to the relevance of the revised Starling Principle in guiding and interpreting the effects of intravenous fluid therapy. The name "Revised Starling Principle" is, however, unfortunate for it implies that the original principle was incorrect and required revising. Perhaps because of this misnomer, the revised Starling Principle has been misunderstood and subsequently misrepresented.

For example, in a recent publication [53] it is said that the revised Principle "has challenged the traditional Starling formula equation", that "the plasma's oncotic pressure is less important than previously thought" and that fluid absorption from the tissues does not occur. It has also been suggested that the "Revised Principle" predicts that the movement of fluid from the interstitial spaces into plasma can only occur via the lymphatics and not by raising the plasma colloid osmotic pressure [53]. All these statements are incorrect.

First, far from challenging the equation which describes the classical Starling Principle, the development uses the traditional equation to show what its

consequences are when the exchange vessels in tissues have a low but finite permeability to macromolecules.

Second, the revised principle does ***not*** say that fluid uptake from the tissues cannot occur. If this were so, it would be difficult to account for fluid uptake from the gastro-intestinal tract or reabsorption of most of the glomerular filtrate in the kidneys, let alone the inconsistency between such a claim and the large body of evidence demonstrating the direct uptake of fluid from the tissues into the blood, including Starling's own experiments. What the revised principle does say is that where the ISF of a tissue is formed entirely from the ultrafiltrate of the plasma flowing through its microcirculation, fluid uptake from tissues directly into blood is always transient. Thus, a fall in the mean microvascular pressure difference across microvascular walls below the effective colloid osmotic pressure difference between plasma and ISF in these tissues results in fluid uptake from ISF directly into the circulating plasma but the rate of fluid uptake diminishes with time and eventually reverts to a low level of filtration. The revised principle argues that in these tissues, steady states of blood-tissue fluid exchange are established only when there is at least a very low level of net filtration of plasma into tissues. This is an obvious conclusion since in this type of tissue where all the ISF is generated by filtration from the plasma. The volume of the ISF here is maintained by a low level of filtration into the tissue, which is matched by the flow of lymph out of the tissue. These tissues include both skeletal and smooth muscle, skin and connective tissues and constitute a large fraction of the body mass. In tissues where the source of some ISF is a protein free secretion from adjacent epithelia (eg in the intestinal mucosa and the post glomerular renal microcirculation) steady state conditions of fluid uptake can occur (as discussed in section on "Steady state fluid uptake in specialized tissues").

Third, following on from this, the revised Starling Principle does **not** suggest that raising the colloid osmotic pressure of plasma is an unimportant method for moving fluid from ISF into plasma. This, of course, increases the effective colloid osmotic pressure difference across microvascular walls and if this difference now exceeds the difference in hydrostatic pressures, fluid should flow from tissues into circulating blood.

Perhaps the most important contribution that the Revised Principle might make to peri-operative care lies not so much in the detail of the steady state relations or even the recognition that there often are differences between the mean colloid osmotic pressure of the ISF and that of the peri-capillary fluid but by the graphical analysis used to demonstrate that fluid exchange is determined by $\boldsymbol{\Delta P - \sigma \Delta \Pi}$ as Starling recognized. When this difference is positive, fluid is filtered from the circulation into the tissues. When the difference is negative, fluid is absorbed into the plasma from the tissues. The rates of filtration and absorption are directly proportional to these differences and serve to return fluid exchange to the point on the steady state curve at that value of ΔP. While ΔP in the different tissues cannot be measured, their presence cannot be neglected when trying to interpret changes following intravenous infusions. To illustrate this, we consider a question central to the controversy of whether intravenous infusion of crystalloid solutions is more effective in expanding plasma volume of patients with severe blood loss than it appears to be in normovolemic subjects.

Consider first a healthy volunteer in a supine resting position, in whom Π_P has an initial value of 25 mm Hg and the mean value of P_C is 23 mm Hg. If a purely crystalloid solution is intravenously infused in this subject, it dilutes the plasma protein, decreasing Π_P, and increasing $\Delta P - \sigma\Delta\Pi$ and consequently increasing filtration from plasma to tissues. The filtration rate increases further if P_C rises as the blood volume expands, either as a consequence of an increase in cardiac output or of a compensatory vasodilatation (with a reduction of the pre- to post capillary resistance ratio) particularly in skeletal muscle, with its large contribution to the total body mass. Glomerular filtration rate and subsequently urine flow both increase, resulting in the slow excretion of the fluid load. A large number of studies of this kind have been carried out, notably by Hahn and his colleagues and analyzed using their volume kinetics model [54–56].

Anecdotal reports that crystalloid infusions are more effective than this in clinical situations has been supported in a series of trials, which have found that for patients in intensive care, similar hemodynamic measures can be achieved by volumes of crystalloid solutions only slightly greater than those of solutions containing colloids (e.g. [57, 58]). A mechanism for the increased effectiveness of crystalloid infusions under these conditions involves the physiological response to hypovolemia. Hypovolemia triggers vasoconstriction in much of systemic circulation and the consequent increase in precapillary resistance (particularly in skin and muscle) greatly increases the Ra/Rv ratio and lowers P_C (see eq. 2.2 above). The fall in P_C may be increased further by an accompanying fall in P_a with a reduced cardiac output. Such a fall in P_C results in the driving pressure for filtration, $\Delta P - \sigma\Delta\Pi$, becoming negative and consequently fluid moves from ISF into the plasma. These changes are shown in terms of the relations between filtration and absorption rates and P_C in Fig. 2.16a and b. In Fig. 2.16a, the expected changes in filtration rate and P_C are shown following intravenous infusion of crystalloid solution in the healthy normovolemic subject. The vertical arrow, AB, indicates the rise in filtration rate if ΔP remains constant and the line, AC, how this rise may be amplified if, as seems likely, ΔP increases. The changes in the hypovolemic patient are shown in Fig. 2.16b. Here, the effects of the instantaneous vasoconstriction are the same shown as for a step fall in ΔP, previously illustrated in Fig. 2.8. If the vasoconstriction and consequent fall in ΔP occurs more slowly, a curvilinear path might be followed. The upward pointing vertical arrow indicates the effects of either the physiological uptake of fluid from the tissues or infusing a crystalloid solution at constant P_C. Intravenous infusion of crystalloid solutions at this stage not only speeds up this process of restoring the circulating volume but aids its completion. Reports in the older literature indicate that physiological compensation is limited in the short term. Kaufmann and Müller [59] reported that in healthy individuals, estimates of the dilution of the plasma proteins immediately after blood donations of 400 ml, indicated that while 50–60% of the plasma volume was restored in 15 min, no further changes occurred over the subsequent 15 min. The effects of both physiological compensatory fluid uptake and intravenous crystalloid infusions should be the same, diluting the circulating plasma protein concentration and consequently shifting the position of the steady state curve so that its inflexion occurs at a lower value of

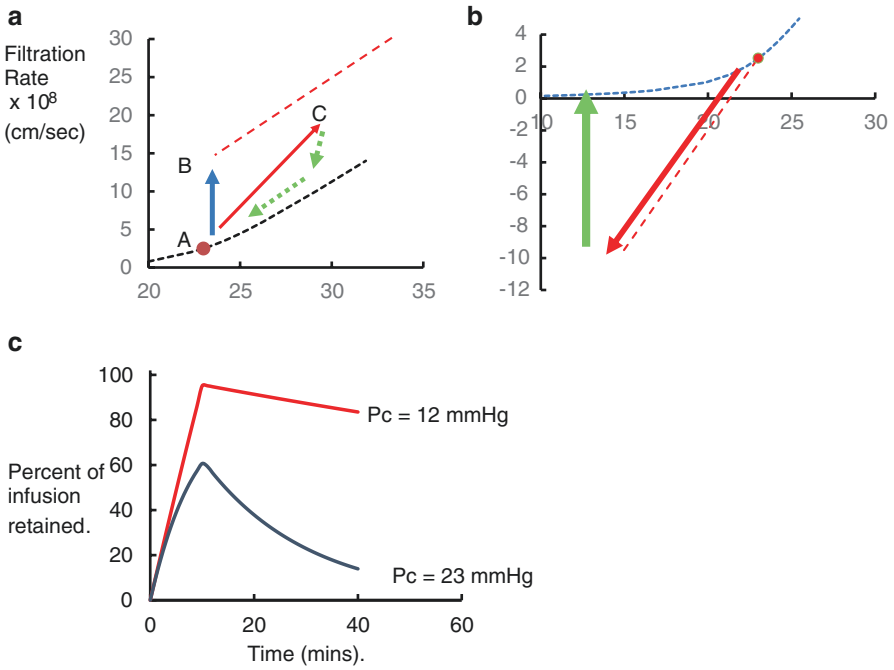

Fig. 2.16 Relationships between microvascular fluid filtration (J_V/A) and microvascular pressure difference (ΔP) before during and following intravenous infusion of an isotonic crystalloid solution. Point A indicates values of J_V and ΔP before infusion and blue arrow, the changes in J_V/A at constant ΔP to point B where infusion ends. If, as is most likely, expansion of the circulating volume leads to vasodilatation, with reduced *Ra/Rv* and a consequent rising P_C, changes in J_V are shown by the red arrow leading towards point C. Green dashed arrows indicate excretion of the fluid load. (**b**) Changes in *Jv/A* in an acutely hypovolemic patient. Initial vasoconstriction with increase in *Ra/Rv,* leads to a rapid fall in Pc with a consequent reversal of fluid filtration to fluid uptake from tissues to plasma (red arrow A to B). If crystalloid solution is infused at B, fluid is retained and plasma volume restored to a degree determined by dilution of plasma proteins to the stage where $\sigma\Delta\Pi = \Delta P$ at the value of *Pc* at point C. Fluid is no longer retained if infusion is continued beyond this stage (**c**) Predictions of the fraction of a crystalloid infusion that is retained in the circulation in a tissue such as muscle at normal and reduced P_C

ΔP. Based on the calculations underlying Fig. 2.16a, b, and assuming the mean value of the product of the hydraulic permeability and exchange surface area for all the microvascular beds of the body is similar to that in human skeletal muscle, the percentage of the infusion which is retained in the circulation over a 40 min period are shown for the healthy subject and the patient in Fig. 2.16c. We have pointed out that in the hypovolemic patient, the infusion of crystalloid solutions has the same effect on Π_P as the physiological compensatory response of absorption of largely protein-free fluid from tissues into the plasma. One big difference, however, is that as Π_P is reduced and $\sigma\Delta\Pi$ falls towards ΔP in the vasoconstricted systemic circulation, the rate of physiological fluid uptake into the plasma also decreases and comes

to halt when $\sigma\Delta\Pi = \Delta P$. Unfortunately, the clinician has no obvious means of knowing when this occurs. In most organs and tissues supplied by the systemic circulation, a low level of edema is reversible but this is not the case for the pulmonary circulation. The greatest risk from over-transfusion is pulmonary edema.

The clinician may, however, be guided by the revised interpretation when considering the effects of fluid therapy on the pulmonary circulation. The lungs of healthy individuals are protected from edema by the low microvascular pressures in pulmonary capillaries (7–10 mm Hg) and by the speed with which transient changes in filtration rate reach new steady state values following small changes in the Starling pressures. In addition to the brisk increase of $\sigma\Delta\Pi$ that follows an increase in filtration rate, there is also a reduction of ΔP since interstitial hydrostatic pressure in the lungs lies normally in the range of −5 to –10 mm Hg (sub-atmospheric) and rises rapidly with expansion of pulmonary interstitial volume acting as an additional buffer against edema formation. The low pulmonary capillary pressures mean that fluid filtration rates sit on the flat region of the steady state curve, 10 mm Hg or more below its upward inflection (similar to point C in Fig. 2.16b). This means that dilution of the plasma proteins during intravenous infusions of crystalloid solutions should have little effect upon pulmonary interstitial volume until the plasma colloid osmotic pressure is reduced to a value just above the mean pulmonary P_C. When large fluid volumes are infused intravenously, a logical precautionary measure might be to monitor patients' plasma protein concentrations, or even better, their plasma colloid osmotic pressures together with pulmonary artery pressure. The infusion of crystalloid could then be discontinued as soon as the colloid osmotic pressure approached 10–12 mm Hg.

Although changes in circulating plasma volume are shown in Fig. 2.16c, it should be remembered that the near constant value maintained for nearly 30 min following a 12 min infusion of crystalloid solution when P_C = 12 mm Hg is predicted on the assumption that P_C remains low and all micro-vessels have the same permeability properties to fluid and macromolecules as those found in skeletal muscle of healthy subjects. This, of course, is, at best, an approximation. Until there is a more complete quantitative understanding of the dynamics of blood volume regulation and methods available for assessing this in the operating room, predictions of the effects of intravenous infusions are at best imprecise. At present, there is no easy way for the clinician to know the value of the mean P_C in most major components of the systemic circulation.

A Note on the Measurements of Changes in Plasma Volume

To manage intravenous fluid therapy efficiently one should have a rapid and reliable method for estimating changes in plasma volume. Unfortunately, there is no method of this kind available. Whereas plasma volume can be estimated from the dilution of a labeled plasma protein, the time taken for the tracer to mix sufficiently to reach a uniform concentration within circulation is sufficient for a significant fraction of tracer to have left the plasma and entered the tissues. To remedy this, serial

measurements of plasma tracer concentration are made and once they are seen to follow a steady exponential decline, back-extrapolation to zero time (the time of injection) provides a value of concentration that can be taken to represent that which would be present when the injected mass of tracer was uniformly distributed throughout the plasma volume. Hence if m is the amount of tracer injected into the circulation, C_0 is the concentration at zero time and V_P is the plasma volume, then $V_P = m/C_0$. This is not a method that can be used to estimate rapidly changing plasma volumes and most investigators have instead used changes of hematocrit as an index of the relative changes in plasma volume when total red cell volume in the circulation is considered to be constant. This may seem to be a reasonable approach but it involves major uncertainties. Before considering these, let us revise the basic idea of the method. Let H be the hematocrit and V_C and V_P are the total circulating volumes of the red cells and plasma, it seems reasonable to say:

$$\frac{H}{100} = \frac{V_C}{V_C + V_P}, \text{and}$$

$$\frac{100}{H} = \frac{V_C + V_P}{V_C} = 1 + \frac{V_P}{V_C} \tag{2.6}$$

Let H_1 be the hematocrit of a sample of blood taken from a patient before a procedure and H_2 be its value 40 min after infusion of 500 ml of a crystalloid solution. Providing the total volume of circulating red cells has remained unchanged, the ratio of the plasma volumes corresponding to H_1 and H_2 is calculated from eq. (2.6) as:

$$\frac{\frac{100}{H_2} - 1}{\frac{100}{H_1} - 1} = \frac{V_{P2}}{V_C} \cdot \frac{V_C}{V_{P1}} = \frac{V_{P2}}{V_{P1}} \tag{2.7}$$

The relative change in plasma volume is:

$$\frac{V_{P2} - V_{P1}}{V_{P1}} = \frac{V_{P2}}{V_{P1}} - 1 = \frac{(100/H_2) - 1}{(100/H_1) - 1} - 1 \tag{2.8}$$

If, initially, the total volumes of circulating plasma and cells are 3 L and 2 L respectively and 300 ml of the infused 500 ml of crystalloid solution is retained when the blood has a hematocrit of H_2, then V_{P2}/V_{P1} should equal 1.1, and plasma volume would be 3.3 liters. If H_1 was 40% then H_2 should be 37.7%. With an error of 1% in the estimation of hematocrit, H_1 could be 41% and H_2 = 37%. Using these slightly erroneous values, the relative change in plasma volume would be estimated as 1.183. With an initial plasma volume of 3 L, the measured change of hematocrit would now suggest the plasma volume was 3.550 L, an overestimate of 250 ml and a plasma volume 50 ml greater than the infused volume. This calculation emphasizes how very small errors in the measurement of hematocrit lead to large errors in

the interpretation of changes in plasma volume. Obviously, such errors can be minimized by making multiple determinations of hematocrit on each blood sample.

A second problem, when estimating changes of plasma volume from changes in hematocrit, arises from the differences between the hematocrit determined on blood taken from a large vessel and that calculated from measurements of the total plasma volume and total red cell volume, the whole body hematocrit. In most individuals the large vessel hematocrit (H_{LV}) is greater than the whole body hematocrit (H_M), with the ratio of H_M/H_{LV} (described as the F-cell ratio) falling between 0.88 and 0.94 for most healthy (and non-pregnant) adults [60–63]. In pregnancy (where maternal blood volume is expanded) the ratio falls and in the new born it may be as low as 0.8 [60]. Variations in the ratio in the same individual occur from time to time and it is suggested that these are associated with the redistribution of blood in the systemic circulation [64]. Thus estimates of changes of plasma volume with acute changes in posture using dye dilution have been reported to be twice as great as those made from changes in hematocrit [64].

A contributing factor is that red cells circulate through most peripheral circulations more rapidly than plasma and that rather than representing the ratio of the volume of red cells to the volume of blood, the hematocrit in large vessels reflects the ratio of the flow of cells to the flow of blood. The flows of red cells and plasma are related to their overall volumes through their mean transit times. If τ_c and τ_p are transit times for the red cells and the plasma respectively, then eq. (2.6) may be rewritten as:

$$\frac{100}{H_{LV}} = 1 + \frac{V_P}{V_C}\frac{\tau_C}{\tau_P} \tag{2.9}$$

When a change of plasma volume is calculated from eq. (2.7), the result becomes:

$$\frac{\left[\left(100/H_1\right)-1\right]}{\left[\left(100/H_2\right)-1\right]} - 1 = \frac{V_{P2}}{V_{P1}} \cdot \frac{\tau_{C2}}{\tau_{C1}} \cdot \frac{\tau_{P1}}{\tau_{P2}} - 1 \tag{2.10}$$

where subscripts 1 and 2 represent the initial and final volumes and transit times respectively. Only if the ratio τ_c/τ_p remains unchanged will the estimate of a change in V_p be correct. A small change in the value of τ_c/τ_p accompanying a change in V_P can lead to misinterpretation.

This can be illustrated by the following numerical example. If the intravenous infusion of a fluid increases V_P from 3.0 to 3.5 l and is accompanied by an increase in red cell velocity relative to plasma velocity, reducing τ_c/τ_p from 0.9 to 0.85, by ignoring the transit time ratios one might conclude that the increase in plasma volume was 306 ml instead of 500 ml; i.e., an underestimate of just under 40%. If, by contrast, the red cell velocity was slowed by the infusion, increasing τ_c/τ_p from 0.9 to 0.95, ignoring this change would suggest that the increase in plasma volume was 694 ml—an overestimate of nearly 40%. This margin of error indicates that small changes in the relative transit times of red cells and plasma in the circulation can compromise estimates of changes in plasma volume following the intravenous infusion of fluids. The message from this is that estimates of changes in plasma volume

based on changes in large vessel hematocrit should be regarded with critical caution [64].

Conclusion

The so-called "revised Starling Principle" develops the interpretation of Starling's Hypothesis in two ways. First it recognizes that the permeability of microvascular walls to macromolecules means that there is never an equilibrium between the hydrostatic and colloid osmotic pressure between the plasma and interstitial fluid. The colloid osmotic pressure difference is itself dependent on filtration of fluid from plasma into the tissues, and fluid uptake from ISF to plasma can only occur transiently in tissues where the ISF is formed entirely as a plasma filtrate. Steady state uptake of fluid into the circulation occurs only in those tissues where a large component of the ISF is a protein-free secretion from a neighboring epithelium or where the ISF flows through the tissue as in lymph nodes.

The second way in which the revised principle develops the classical hypothesis is that it recognizes that the difference in colloid osmotic pressure holding fluid within the vascular system is not between that of the plasma and its mean value for ISF but the difference across the primary ultra-filtering structure within microvascular walls. This is the glycocalyx at the luminal surface of endothelium. In vessels with continuous (non-fenestrated) endothelia, the low flux of macromolecules, which cross the endothelium by breaches in the glycocalyx, are prevented from back-diffusing from the basement membrane to the underside of the glycocalyx by a low level of filtration, the velocity of which is amplified a hundredfold during its passage through the narrow breaks in the junctional strands. As a consequence, the relevant effective osmotic pressure across the glycocalyx differs from the difference in colloid osmotic pressure between that of the plasma and its mean value for the interstitial fluid.

When plasma colloid osmotic pressure, Π_P, is constant, changes in net fluid transport rates are transiently directly proportional to step changes in hydrostatic pressures. With different time courses in different tissues, these initial rates move toward steady state values. Graphs relating steady state fluid transport to microvascular pressures in most tissues (e.g., muscle, skin, connective tissues) are not linear, showing a marked inflection when microvascular pressures are close to plasma colloid osmotic pressure. As pressure rises between 0 and Π_P, fluid filtration is very small and difficult to detect; when pressure is greater than Π_P, filtration rate rises sharply, and with further increases in pressure becomes linear with a slope equal to the hydraulic permeability of the microvascular wall. This nonlinear behavior of steady state fluid exchange is of potential importance in guiding intravenous fluid therapy. It predicts that the effects of dilution of the plasma proteins and reduction of Π_P on blood-tissue fluid exchange are different when microvascular pressure (P_C) is in the range of Π_P and when P_C is well below this. When P_C is initially equal to or greater than Π_P, dilution of the plasma increases filtration into tissues; when P_C is well below Π_P, dilution of the plasma proteins has little effect. This is because

the steady state filtration rates at normal and reduced Π_P differ by very little until Π_P falls to within a couple of mm Hg of the low P_C. Low values of P_C occur in muscle with intense peripheral vasoconstriction (e.g., following blood loss) and are also normally present in pulmonary capillaries. This suggests that monitoring Π_P may help to avert pulmonary edema during infusions of large volumes of crystalloids.

Appendix

Some readers may be interested to follow the theoretical derivation of the steady state relation between fluid filtration through a membrane and the pressure difference across the membrane when the solute responsible for an osmotic pressure difference opposing filtration has a reflection coefficient of less than one.

The rate of transport of the solute through the membrane is J_S and transport occurs by convection (fluid filtration per unit area of membrane = J_V) and diffusion (diffusion coefficient of the solute in the membrane water = D). If the overall thickness of the membrane between its upstream and downstream surfaces = Δ and x = any distance measured in the membrane from the upstream surface between 0 and Δ, the flux of solute at x is given by:

$$J_S = J_V\left(1-\sigma\right)C(x) + D\left(-\frac{dC(x)}{dx}\right),$$

Where C(x) is solute concentration at x. Rearranging this expression leads to:

$$\frac{dC\left(x\right)}{dx} = \frac{J_v\left(1-\sigma\right)}{D}\mathrm{C}\left(\mathrm{x}\right) - \frac{J_S}{D}. \tag{2.11}$$

Both J_S and J_V are time invariant in the steady state and σ and D are constants; defining $a = J_V(1-\sigma)/D$ and $b = J_S/D$, allows simplification of 2.1A to:

$$\frac{dC\left(x\right)}{dx} = a.C\left(x\right) - b. \tag{2.12}$$

When x = 0, C(x) = C_1 the concentration of solute as the solution enters the membrane; when x = X, C(x) = C_2, the concentration solute in the ultrafiltrate leaving the membrane. Integrating eq. (2.12) between the limits of 0 and X:

$$\int_0^X \frac{dC\left(x\right)}{\left(aC\left(x\right)-b\right)} = \int_0^X dx \,\text{leads to}:$$

$$\ln\frac{\left(aC_2-b\right)}{\left(aC_1-b\right)} = aX, \,\text{which may be written as}:$$

$$\mathrm{a}C_2 - b = \left(aC_1 - b\right)e^{aX}. \tag{2.13}$$

The exponent, aX, is the ratio of the convective velocity of the solute through the membrane to its diffusion velocity and is known as the Péclet number, Pe. In the steady state, the ratio $J_S/J_V = C_2$, and dividing eq. (2.13) through by a and expressing the full meaning of a and b leads to:

$$C_2 = C_1 e^{Pe} - \frac{b}{a}\left(e^{Pe} - 1\right) = C_1 e^{Pe} - C_2 \frac{\left(e^{Pe} - 1\right)}{\left(1 - \sigma\right)},$$

Which can be reduced to:

$$\frac{C_1}{C_2} = \frac{\left(e^{Pe} - \sigma\right)}{\left(1 - \sigma\right)e^{Pe}}. \tag{2.14}$$

Dividing the RHS of 2.4 through by e^{Pe} and inverting yield

$$\frac{C_2}{C_1} = \frac{\left(1 - \sigma\right)}{\left(1 - \sigma e^{-Pe}\right)} \tag{2.15}$$

The concentration difference across the membrane is:

$$C_1 - C_2 = C_1 \sigma \frac{\left(1 - e^{-Pe}\right)}{\left(1 - \sigma e^{-Pe}\right)} \tag{2.16}$$

If we assume the osmotic pressures of the solutions at the upstream surface and leaving the membrane downstream are directly proportional to their solute concentrations, the difference in osmotic pressure opposing filtration, $\Delta\Pi$, can be expressed in terms of the upstream osmotic pressure, Π_1,

$$\Delta\Pi = \Pi_1 \sigma \frac{\left(1 - e^{-Pe}\right)}{\left(1 - \sigma e^{-Pe}\right)} \tag{2.17}$$

For fluid filtration through microvascular walls, Π_1 is equivalent to Π_P, the plasma colloid osmotic pressure, so that the steady state relation between fluid filtration and microvascular pressure difference can be written (approximately) as:

$$J_V = L_P \left[\Delta P - \sigma^2 \Pi_P \frac{\left(1 - e^{-Pe}\right)}{\left(1 - \sigma e^{-Pe}\right)} \right]. \tag{2.18}$$

Equation (2.19) resembles eqs. (2.1) and (2.3) but because Pe is a function of J_V the equation should be written as an expression for ΔP in terms of J_V.

$$\Delta P = \frac{J_V}{L_P} + \sigma^2 \Pi_P \frac{\left(1 - e^{-Pe}\right)}{\left(1 - \sigma e^{-Pe}\right)} \tag{2.19}$$

When appropriate values for the permeability coefficients are substituted into eq. (2.19), non-linear curves similar to those shown in Figs. 2.6, 2.7 and 2.14a can be

constructed. Equations (2.18) and (2.19) are approximations because the assumption made in eq. 2.17 is only approximately true as the relation between osmotic pressure and concentration for macromolecular solutions is not linear but its slope increases with concentration and it is best described by a polynomial expression. To obtain more accurate predictions, numerical solutions can be used to estimate the osmotic pressure difference from the difference in concentration.

References

1. Bayliss WM. Intravenous injection in wound shock: being the Oliver-Sharpey lectures delivered before the Royal College of Physicians of London in May 1918. London, New York etc: Longmans, Green, and Co; 1918.
2. Starling EH. On the absorption of fluids from connective tissue spaces. J Physiol. 1896;19:312–26.
3. Van der Kloot W. William Maddock Bayliss's therapy for would shock. Notes and Records of the Royal Society. 2010;64:271–86.
4. Woodcock TE, Woodcock TM. Revised Starling equation and the glycocalyx model of transvascular fluid exchange: an improved paradigm for prescribing intravenous fluid therapy. Br J Anaesth. 2012;108:384–94.
5. Barcroft H. Bayliss-Starling memorial lecture 1976. Lymph formation by secretion of filtration? J Physiol. 1976;260:1–20.
6. Michel CC. Starling: the formulation of his hypothesis of microvascular fluid exchange and its significance after 100 years. Exp Physiol. 1997;82(1):1–30.
7. Krogh A. Anatomy and physiology of capillaries. Lecture IX. New Haven: Yale University Press; 1922. p. 206–9.
8. Landis EM. Microinjection studies of capillary permeability. II. The relation between capillary pressure and the rate of which fluid passes through the walls of single capillaries. Am J Phys. 1927;82(2):217–38.
9. Krogh A. Anatomy and physiology of capillaries. New Edition. Lecture XII. New Haven: Yale University Press; 1930. p. 312–29.
10. Landis EM. Micro-injection studies of capillary blood pressure in human skin. Heart. 1930;15:209–28.
11. Starling EH. The production and absorption of lymph. In: Schafer EA, editor. Textbook of physiology, vol. 1. London: Pentland; 1898. p. 285–311.
12. Landis EM, Pappenheimer JR. Ch 29. Exchange of substances through the capillary walls. In: Hamilton WF, Dow P, editors. Handbook of physiology. Circulation, vol. 2, sec 2. Washington, DC: American Physiological Society; 1963. p. 961–1034.
13. Levick JR, Michel CC. The effects of position and skin temperature on the capillary pressure in the fingers and toes. J Physiol. 1978;274:97–109.
14. Mahy IR, Tooke JE, Shore AC. Capillary pressure during and after incremental venous elevation in man. J Physiol. 1995;485:213–9.
15. Levick JR. Chapter 11, An introduction to cardiovascular physiology, 5E. London: Hodder Arnold; 2010. p. 198–202.
16. Levick JR. An analysis of the interaction between interstitial plasma protein. Interstitial flow and fenestral filtration and its application to synovium. Microvasc Res. 1994;47:90–124.
17. Landis EM, Gibbon JH. The effects of temperature and tissue pressure on the movement of fluid through the human capillary wall. J Clin Invest. 1933;12:105–38.
18. Pappenheimer JR, Soto-Rivera A. Effective osmotic pressure of the plasma proteins and other quantities associated with the capillary circulation in the hind limbs of cats and dogs. Am J Phys. 1948;152:471–91.

19. Öberg B. Effects of cardiovascular reflexes on net capillary fluid transfer. Acta Physiol Scand. 1964;62(Suppl):229.
20. Mellander S, Öberg B, Odelram H. Vascular adjustments to increased transmural pressure in cat and man with special reference to shifts in capillary fluid transfer. Acta Physiol Scand. 1964;61:34–48.
21. Folkow B, Mellander S. Measurements of capillary filtration coefficient and its use in studies of the control of capillary exchange. In: Crone C, Lassen NA, editors. Capillary permeability. Munksgaard: Proceedings of the Alfred Benzon Symposium II; 1970. p. 614–23.
22. Staverman AJ. The theory of measurement of osmotic pressure. Recl Trav Chim Pays-Bas. 1951;70:344–52.
23. Kedem O, Katchalsky A. Thermodynamic analysis of the permeability of biological membranes to non-electrolytes. Biochim Biophys Acta. 1958;27:229–45.
24. Michel CC. The flow of water through the capillary wall. In: Ussing HH, Bindslev N, Lassen NA, Sten-Knudsen, editors. Alfred Benzon Symposium 15: Water transport across epithelia. Copenhagen: Munksgaard; 1981. p. 268–79.
25. Michel CC, Kendall S. Differing effects of histamine and serotonin on microvascular permeability in anaesthetized rats. J Physiol. 1997;501:657–62.
26. Guyton AC. A concept of negative interstitial pressure based on pressures in implanted perforated capsules. Circ Res. 1963;12:399–415.
27. Scholander PF, Hargens AR, Miller SL. Negative pressure in the interstitial fluid of animals. Science. 1968;161:321–8.
28. Wiederhielm CA, Weston BV. Microvascular, lymphatic and tissue pressures in the unanesthetized mammal. Am J Phys. 1973;225:992–6.
29. Aukland K, Fadnes HO. Protein concentration of interstitial fluid collected from rat skin by a wick method. Acta Physio Scand. 1973;88:350–8.
30. Brace RA, Guyton AC. Interaction of transcapillary Starling forces in the isolated dog forelimb. Am J Phys. 1977;233:H136–40.
31. Chen HI, Granger HG, Taylor AE. Interaction of capillary, interstitial and lymphatic forces in the canine hind paw. Circ Res. 1976;39:245–54.
32. Michel CC. Fluid movements through capillary walls. In: Renkin EM, Michel CC, editors. Handbook of physiology. The cardiovascular system, Microcirculation, part 1, vol. 4. Bethesda, MD: American Physiological Society; 1984. p. 375–409.
33. Taylor AE, Townsley MI. Evaluation of Starling's fluid flux equation. News Physiol Sci. 1987;2:48–52.
34. Levick JR. Capillary filtration-absorption balance reconsidered in the light of extravascular factors. Exp Physiol. 1991;76:825–57.
35. Levick JR, Michel CC. Microvascular fluid exchange and revised Starling principle. Cardiovasc Res. 2010;87:198–210.
36. Hu X, Weinbaum S. A new view of Starling's hypothesis at the microstructural level. Microvasc Res. 1999;58:281–304.
37. Michel CC, Phillips ME. Steady state fluid filtration at different capillary pressures in perfused frog mesenteric capillaries. J Physiol. 1987;388:421–35.
38. Michel CC. Exchange of fluid and solutes across microvascular walls. In: Seldin, Giebisch, editors. The kidney: Physiology and pathophysiology, vol. 1. Philadelphia, Pennsylvania: Academic; 2013. p. 263–90.
39. Kajimura M, Wiig H, Reed RK, Michel CC. Interstitial fluid pressure surrounding rat mesenteric venules during changes in fluid filtration. Experimental Physiol. 2001;86:33–8.
40. MacPhee PJ, Michel CC. Fluid uptake from the renal medulla into the ascending vasa recta in anaesthetised rats. J Physiol. 1995;487:169–83.
41. Pallone TL, Turner MR, Edwards A, Jamison RL. Countercurrent exchange in the renal medulla. Am J Physiol Regul Integr Comp Physiol. 2003;284:1153–75.
42. Wang W, Michel CC. Modeling exchange of plasma proteins between the microcirculation and interstitium of the renal medulla. Am J Phys. 2000;279:F334–44.

43. Adair TH, Guyton AC. Modification of lymph by lymph nodes. II. Effect of increased lymph node venous pressure. Am J Phys. 1983;245:H616–22.
44. Weinbaum S. Distinguished lecture. Models to solve the mysteries of biomechanics at cellular level. A new view of fiber-matrix layers. Ann Biomed Eng. 1998;26:627–43.
45. Michel CC. Microvascular fluid filtration and lymph formation. In: Santambrogio L, editor. Immunology of the lymphatic system. New York: Springer; 2013. p. 35–51.
46. Hu X, Adamson RH, Lui B, Curry FE, Weinbaum S. Starling forces that oppose filtration after tissue oncotic pressure is increased. Am J Phys. 2000;279:H1724–36.
47. Adamson RH, Lenz JF, Zhang X, Adamson GN, Weinbaum S, Curry FE. Oncotic pressures opposing filtration across non-fenestrated rat microvessels. J Physiol. 2004;557:889–907.
48. Zhang X, Adamson RH, Curry FE, Weinbaum S. Transient regulation of transport by pericytes in venular microvessels via trapped microdomains. Proc Natl Acad Sci U S A. 2008;105:1374–9.
49. Zweifach BW, Lipowsky HH. Pressure flow relations in the blood and lymph microcirculations. In: Renkin EM, Michel CC, editors. Handbook of physiology. Section 2, vol. 4, Part iv. Washington, DC: American Physiological Society; 1984. p. 257–307.
50. Olszewski WL, Engeset A, Sokolowski J. Lymph flow and protein in the normal male leg during lying, getting up, and walking. Lymphology. 1977;10:178–83.
51. Knox P, Pflug JJ. The effect of the canine popliteal node on the composition of lymph. J Physiol. 1983;345:1–14.
52. Bates DO, Levick JR, Mortimer PS. Starling pressures in the human arm and their alterations in post-mastectomy oedema. J Physiol. 1994;447:355–63.
53. Zdolsek M, Hahn RG, Zdolsek JH. Recruitment of extravascular fluid by hypertonic albumin. Acta Anaesthesiol Scand. 2018;62:1255–60.
54. Stahle L, Nilsson A, Hahn RG. Modelling the volume of expandable fluid spaces during intravenous fluid therapy. Br J Anaesth. 1997;78:138–43.
55. Drobin D, Hahn RG. Volume kinetics of ringer in hypovolemic volunteers. Anesthesiology. 1999;90:81–91.
56. Hahn RG. Volume kinetics for infusion fluids. Anesthesiology. 2010;113:470–81.
57. Bayer O, Reinhardt K, Kohl M, Kabisch B, Marshall J, Sakr Y, et al. Effects of fluid resuscitation with synthetic colloids or crystalloids alone on shock reversal, fluid balance and patient outcomes in patients with severe sepsis: a prospective sequential analysis. Crit Care Med. 2012;40:2543–51.
58. Jabaley C, Dudaryk R. Fluid resuscitation for trauma patients: crystalloids versus colloids. Curr Anesthesiol Rep. 2014;4:216–24.
59. Kaufmann VW, Müller AA. Expansion des Plasmavolumens nach rascher Verminderung der zirkulierenden Blutmenge. Z Kreislaufforsch. 1958;47:719–31.
60. Lawson HC. The volume of blood – a critical examination of methods for its measurement. In: Hamilton WF, Dow P, editors. Handbook of physiology, Section 2, vol. 1. Washington DC: American Physiological Society; 1962. p. 23–49.
61. Retzlaff JA, Tauxe WN, Kiely JM, Stroebel KF. Erythrocyte volume, plasma volume and lean body mass in adult men and women. Blood. 1969;33:649–67.
62. Harrison MH. Effects of thermal stress and exercise on blood volume in humans. Physiol Rev. 1985;65:149–209.
63. Sawka MN, Young AJ, Pandolf KB, Dennis RC, Valeri CR. Erythrocyte, plasma, and blood volume of healthy young men. Med Sci Sports Exercise. 1991;24:447–53.
64. Johansen LB, Vidabaek R, Hammerum M, Norsk P. Under estimation of plasma volume changes in humans by hematocrit/haemoglobin method. Am J Physiol. 1998;274 (Regulatory Integrative Comp. Physiol 43):R126–30.